

Article

Estimation of Activity and Molar Excess Gibbs Energy of Binary Liquid Alloys Pb-Sn, Al-Sn and In-Zn from the Partial Radial Distribution Function Simulated by Ab Initio Molecular Dynamics

Tianao Zhang ¹, Xiumin Chen ^{2,3}, Yi Lu ^{1,4}, Jiulong Hang ¹ and Dongping Tao ^{1,*}

¹ Faculty of Metallurgical and Energy Engineering, Kunming University of Science and Technology, Kunming 650093, China; zhtiao2021@163.com (T.Z.); 17313656732@163.com (Y.L.); 17852587095@163.com (J.H.)

² National Engineering Research Center of Vacuum Metallurgy, Kunming University of Science and Technology, Kunming 650093, China; chenxiumin9@outlook.com

³ Key Laboratory for Nonferrous Vacuum Metallurgy of Yunnan Province, Kunming University of Science and Technology, Kunming 650093, China

⁴ State Key Laboratory of Complex Nonferrous Metal Resources Clean Utilization, Kunming University of Science and Technology, Kunming 650093, China

* Correspondence: dongpingt@aliyun.com

Abstract: For the present, it is difficult to obtain thermodynamic data for binary liquid alloys by experimental measurements. In this study, the molecular dynamics processes of the binary liquid alloys Pb50-Sn50, Al50-Sn50, and In50-Zn50 were simulated by using the ab initio molecular dynamics (AIMD) principle, and their partial radial distribution functions (PRDF) were obtained at different simulation steps. Combined with the relevant binary parameters of the Molecular Interaction Volume Model (MIVM), Regular Solution Model (RSM), Wilson Model, and Non-Random Two-Liquid (NRTL) models. The integral terms containing the PRDF were computed using the graphical integration method to obtain the parameters of these models, thus estimating their activity and molar excess Gibbs energy. The total average relative deviations (ARD) of the activity and molar excess Gibbs energy estimates of the four models for the binary liquid alloys Pb50-Sn50, Al50-Sn50, and In50-Zn50 at full concentration when the PRDF is obtained by the symmetry method are MIVM: 21.59% and 59.35%; RSM: 21.63% and 60.27%; Wilson: 24.27% and 86.7%; NRTL: 23.9% and 83.24%. When the PRDF is obtained by the asymmetric method: MIVM: 22.86% and 68.08%; RSM: 32.84% and 68.66%; Wilson: 25.14% and 82.75%; NRTL: 24.49% and 85.74%. This indicates that the estimation performance of the MIVM model is superior to the other three models, and the symmetric method performs better than the asymmetric method. The present study also derives and verifies the feasibility of Sommer's equation for estimating the molar excess Gibbs energy and activity of binary liquid alloy systems in the Miedema model by using different equations of enthalpy of mixing versus excess entropy given by Tanaka, Ding, and Sommer. The total ARD of Tanaka, Ding, and Sommer's relational equations in the Miedema model for estimating the activities and molar excess Gibbs energies of the binary liquid alloys Pb-Sn, Al-Sn, and In-Zn are 3.07% and 8.92%, 6.09% and 17.1%, and 4.1% and 14.77%. The results indicate that the estimation performance of the Miedema model is superior to the other four models.

Keywords: binary liquid alloys; thermodynamic modeling; activity; partial radial distribution function (PRDF); ab initio molecular dynamics simulation (AIMD)



Citation: Zhang, T.; Chen, X.; Lu, Y.; Hang, J.; Tao, D. Estimation of Activity and Molar Excess Gibbs Energy of Binary Liquid Alloys Pb-Sn, Al-Sn and In-Zn from the Partial Radial Distribution Function Simulated by Ab Initio Molecular Dynamics. *Metals* **2024**, *14*, 102. <https://doi.org/10.3390/met14010102>

Academic Editor: Alain Pasturel

Received: 14 December 2023

Revised: 8 January 2024

Accepted: 12 January 2024

Published: 15 January 2024



Copyright: © 2024 by the authors. Licensee MDPI, Basel, Switzerland. This article is an open access article distributed under the terms and conditions of the Creative Commons Attribution (CC BY) license (<https://creativecommons.org/licenses/by/4.0/>).

1. Introduction

The thermodynamic parameters of solutions are fundamental data for the development of new processes, process optimization, and theoretical research in many fields.

The study of the thermodynamic properties of solutions is essential for metallurgical preparation or the development of new materials. Among them, binary liquid alloys are characterized by simple structure and easy processing, which are widely used in aerospace, automotive, marine, and other fields [1]. Due to the complexity and accuracy limitations of actual high temperature experiments, in many cases, the experimental measurement process is difficult and the thermodynamic data results obtained are not accurate [2,3]. Therefore, it is worthwhile to seek an accurate, convenient, and reasonable method to simulate the experimental part of thermodynamic research. Since most of the actual solutions in thermodynamic experiments are non-ideal solutions, a modified concentration (activity) instead of the actual concentration must be considered to accurately analyze the thermodynamic behavior of the solution when simulating and calculating the thermodynamic parameters [4,5]. Therefore, the activity becomes one of the important research topics in the field of thermodynamic properties, and the molar excess Gibbs energy of the alloy can also be used as a more intuitive comparison and reference for the value of the alloy activity as well as the change of the alloy activity.

Until now, scientists have proposed many methods for calculating activity coefficients, such as the regular solution model (RSM) proposed by Hilderande [6,7] in 1929 and Wilson [8] in 1964, who postulated that interactions between molecules depended mainly on the “local concentration” which could be expressed as a volume fraction, and proposed the Wilson equation. The Non-Random Two-Liquid (NRTL) Model equation proposed by Renon and Prausnitz in 1968 is based on the semiempirical equation for the concept of localized concentration [9]. Miedema et al. developed a semiempirical theoretical model in 1973. Miedema et al. extended the metacellular model used by Wigner–Seitz in the theoretical description of pure metals to binary alloys and developed an empirical model after the gradual improvement of the Miedema model [10,11]. Tao [12] in 2000, based on statistical thermodynamics and fluid phase equilibrium theory, derived a new expression for the regular coordination partition function of liquids and their mixtures. Tao put forward the concept of local coordination number of molecules in liquid mixtures and its expression, thus establishing a new model for the thermodynamics of liquid mixtures that is the Molecular Interaction Volume Model, abbreviated as MIVM, and the above models have been widely used.

Ab initio molecular dynamics (AIMD), also known as first-principles molecular dynamics, has the basic idea of taking the electronic structure of molecules and interatomic interactions as the basis of calculations and calculating the structure and properties of materials through molecular dynamics simulations [13,14]. AIMD calculation methods have a wide range of applications, which can be used to study the structure, thermodynamic properties, kinetic properties, and electronic structure of a variety of materials [15].

Based on the predictive activity models of various binary alloy systems and the principle of AIMD, this paper uses Materials Studio software (Materials Studio 7.0-2020) to construct a binary alloy metal molecular model [16]. Next, Vienna ab initio simulation package (VASP) software (VASP-5.4.1.) is used to simulate molecular dynamics processes to obtain the thermodynamic data required for the binary liquid alloy system, and the partial radial distribution function ($g(r)$) is obtained by Visual Merchandising (VMD) software (VMD-1.9.4a53) [17–20]. Then, the parameters required for the MIVM, RSM, Wilson, and NRTL models are obtained by calculating the potential energy function. Two methods (the PRDF is obtained by the asymmetry method and the PRDF is obtained by the symmetry method) were used to estimate the activity and molar excess Gibbs energy of liquid mixtures of three binary positive deviation systems, Pb50 Sn50, Al50 Sn50, and In50 Zn50. Selection of binary liquid alloys with 50 percent monometallic concentration have a low melting point, good fluidity, easy processing, and low cost. Another task is to estimate the molar excess Gibbs energy and activity of the three systems in the Miedema model using three different relation equations between mixing enthalpy and excess entropy given by Tanaka [21], Ding [22], and Sommer [23,24], and to compare the estimation effects of each model and the two methods.

2. Methods and Steps of Simulation Calculation

2.1. Obtaining the Partial Radial Distribution Function by AIMD

In this work, the simulation uses the AIMD principle. Firstly, the molecular configuration of the alloy cells was established in the Materials Studio simulation software using the Packing method [16]. A total of 118 atoms consisting of 59 Pb atoms and 59 Sn atoms; 126 atoms consisting of 63 Al atoms and 63 Sn atoms; and 122 atoms consisting of 61 In atoms and 61 Zn atoms were simulated by placing them into square cubic boxes with side lengths of 15.5 Å, 15 Å, and 14 Å, respectively. The densities of the three systems of Pb0.5-Sn0.5, Al0.5-Sn0.5, and In0.5-Zn0.5 were 8.632 g/cm³ [25], 4.53 g/cm³ [26], and 6.665 g/cm³, respectively [27]. Next, AIMD simulations based on density functional theory (DFT) were performed using the VASP software [17]. The exchange-correlation function employed the Perdew–Burke–Ernzerhof (PBE) function, which is based on the generalized gradient approximation (GGA) [18]. Ultrasoft pseudopotentials [19] were used. The cutoff energy is chosen to be 1.3 times higher than the maximum cutoff energy provided in the pseudopotential files [17], and the calculation accuracy was chosen to be 10^{−4} eV/Å for the electron step and 10^{−3} eV/Å for the ion step. In simulating the kinetics, the simulation temperatures were set to 1050 K, 973 K, and 730 K, respectively, with the NVT system [20] synthesized using a Nosé–Hoover thermostat for temperature control [28]. The time step was 3 fs and the maximum number of steps for the ion motion was 5000 (15 ps). The K-point is set to the Gamma point [17]. Subsequently, the trajectory file XDATCAR was obtained as an output of the VASP kinetic simulation calculations, which includes the atomic coordinate information output at certain step intervals (i.e., all the atomic coordinate information of the 5000 steps of the performed calculations). Subsequent import into the VMD software allows the direct generation of $g(r)$ images and $g(r)$ coordinate data required for stepwise calculations [29].

2.2. Obtaining the First Peak of the Partial Radial Distribution Function

The partial radial distribution function is a function that describes the distribution state of matter and is used to describe the distribution of particles in space. It is defined as the product of the probability of a particle appearing on the unit sphere around a point in space and the density of the particle distribution on the sphere. The partial radial distribution function is an important manifestation of orderliness in the liquid alloy system. The typical partial radial distribution function is shown in Figure 1 [30,31]. Function in the origin of the coordinates near the existence of a clear peak, the first peak can be expressed and the central atom has interaction around the atom distribution changes [32].

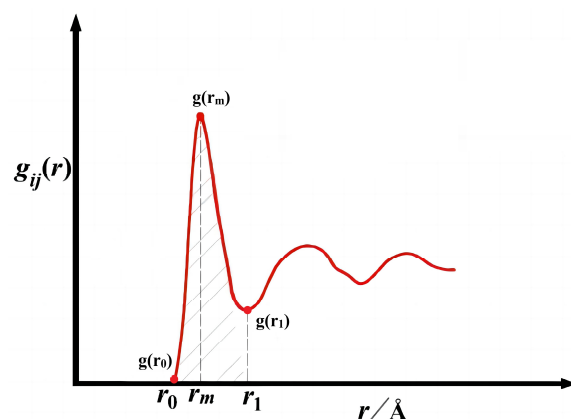


Figure 1. The first valley and first peak of partial radial distribution function.

In this paper, r_0 : represents the abscissa of the starting point of non-zero values; r_1 : denotes the position of the first valley of the function $g_{ij}(r)$; r_m : is the position of the first peak of the function $g_{ij}(r)$; the following $g_{ij}(r) = g_{ji}(r), g_{ii}(r), g_{jj}(r)$ denotes the partial radial distribution function. In this paper, the way of describing the partial radial distribution

function is divided into two kinds: one is the partial radial distribution function in the $r_0 \sim r_m$ region of the integral value of the symmetric treatment to obtain the method called symmetric method; one is to directly select the integral value of the $r_0 \sim r_1$ region of the partial radial distribution function of the method called asymmetric method. The following gives the three systems of all the $g(r)$ images as well as all of the key points of the data in the following Figures 2–4 and Tables 1–3:

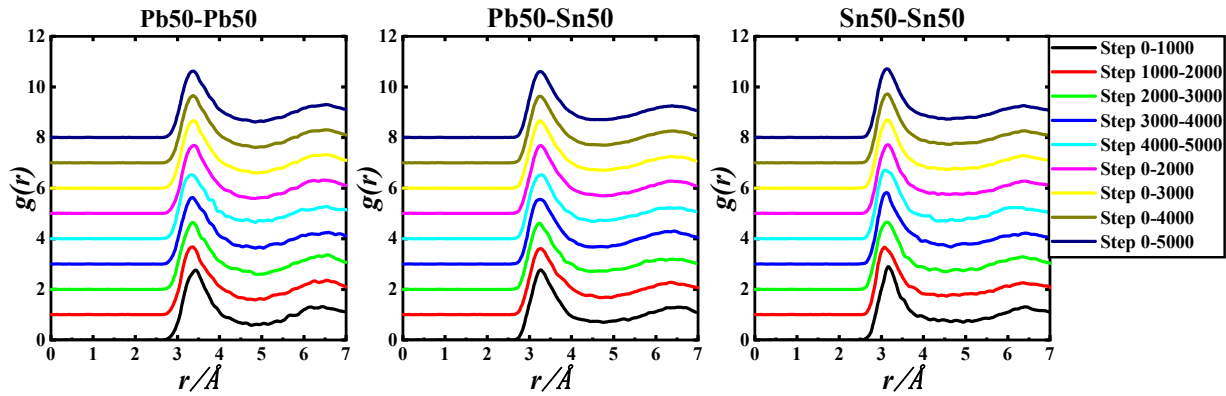


Figure 2. $g_{In-In}(r)$, $g_{In-Zn}(r)$, and $g_{Zn-Zn}(r)$ of the Pb50Sn50-1050 K system based on 5000 step PRDF data.

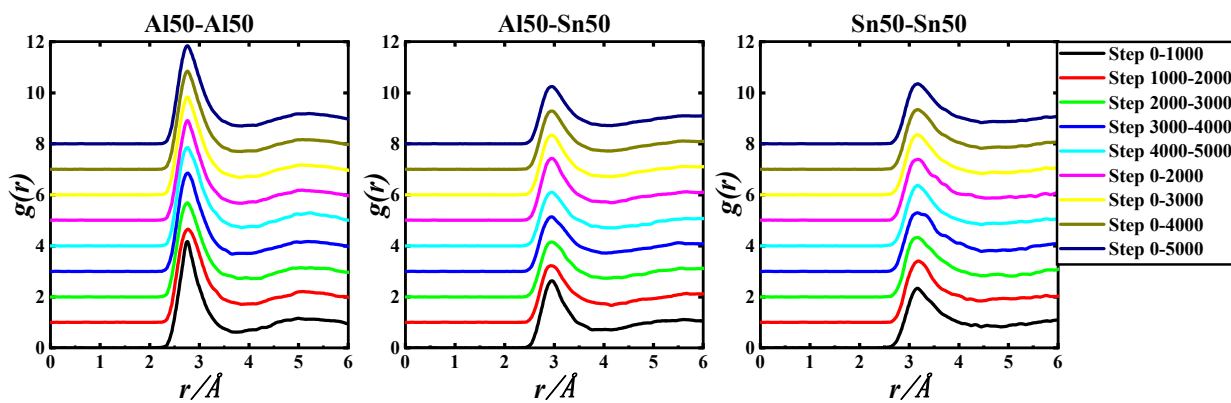


Figure 3. $g_{Al-Al}(r)$, $g_{Al-Sn}(r)$, and $g_{Sn-Sn}(r)$ of the Al50Sn50-973 K system based on 5000 step PRDF data.

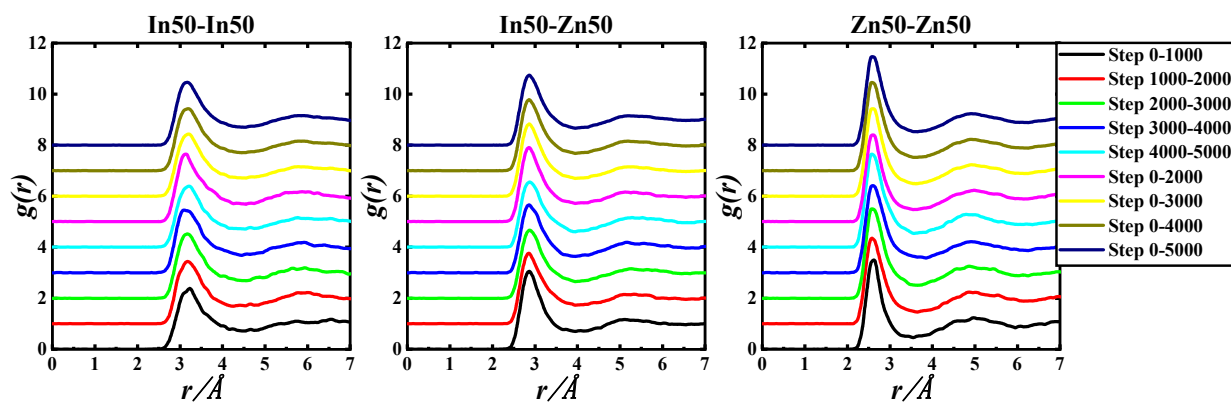


Figure 4. $g_{In-In}(r)$, $g_{In-Zn}(r)$, and $g_{Zn-Zn}(r)$ of the In50Zn50-730 K system based on 5000 step PRDF data.

Table 1. The three key coordinate points of $g_{Pb-Pb}(r)$, $g_{Pb-Sn}(r)$, and $g_{Sn-Sn}(r)$ in the Pb50Sn50-1050 K system.

Parameters	Step of Pb50-Sn50 (1050 K)								
	0–1000	1000–2000	2000–3000	3000–4000	4000–5000	0–2000	0–3000	0–4000	0–5000
$r_{0\ i-i}$	2.650	2.650	2.650	2.650	2.650	2.650	2.650	2.650	2.650
$g(r_{0})_{i-i}$	0.004	0.004	0.004	0.004	0.005	0.004	0.004	0.004	0.004
$r_{m\ i-i}$	3.450	3.350	3.350	3.350	3.350	3.350	3.350	3.350	3.350
$g(r_m)_{i-i}$	2.751	2.671	2.634	2.628	2.521	2.645	2.641	2.638	2.615
$r_{1\ i-i}$	4.750	4.850	4.850	4.550	4.850	4.750	4.850	4.850	4.850
$g(r_1)_{i-i}$	0.577	0.581	0.594	0.680	0.646	0.590	0.595	0.604	0.613
$r_{0\ i-j}$	2.550	2.650	2.550	2.650	2.550	2.550	2.550	2.550	2.550
$g(r_0)_{i-j}$	0.002	0.011	0.001	0.007	0.001	0.001	0.001	0.001	0.001
$r_{m\ i-j}$	3.250	3.250	3.250	3.250	3.250	3.250	3.250	3.250	3.250
$g(r_m)_{i-j}$	2.748	2.601	2.614	2.547	2.508	2.675	2.654	2.627	2.603
$r_{1\ i-j}$	4.750	4.950	4.450	4.450	4.550	4.750	4.750	4.750	4.750
$g(r_1)_{i-j}$	0.699	0.671	0.704	0.669	0.677	0.688	0.700	0.696	0.700
$r_{0\ j-j}$	2.550	2.550	2.550	2.450	2.550	2.550	2.550	2.450	2.450
$g(r_0)_{j-j}$	0.003	0.002	0.013	0.001	0.001	0.002	0.006	0.001	0.001
$r_{m\ j-j}$	3.150	3.050	3.150	3.150	3.050	3.150	3.150	3.150	3.150
$g(r_m)_{j-j}$	2.874	2.632	2.647	2.807	2.667	2.712	2.690	2.719	2.706
$r_{1\ j-j}$	4.150	4.150	4.150	4.650	4.350	4.350	4.150	4.550	4.550
$g(r_1)_{j-j}$	0.790	0.801	0.756	0.673	0.697	0.748	0.783	0.729	0.724

Table 2. The three key coordinate points of $g_{Al-Al}(r)$, $g_{Al-Sn}(r)$, and $g_{Sn-Sn}(r)$ in the Al50Sn50-973 K system.

Parameters	Step of Al50-Sn50 (973 K)								
	0–1000	1000–2000	2000–3000	3000–4000	4000–5000	0–2000	0–3000	0–4000	0–5000
$r_{0\ i-i}$	1.850	2.150	2.250	2.250	2.250	1.850	1.850	1.850	1.850
$g(r_{0})_{i-i}$	0.002	0.001	0.001	0.004	0.005	0.001	0.001	0.001	0.001
$r_{m\ i-i}$	2.750	2.750	2.750	2.750	2.750	2.750	2.750	2.750	2.750
$g(r_m)_{i-i}$	4.165	3.629	3.686	3.843	3.850	3.897	3.827	3.831	3.834
$r_{1\ i-i}$	3.750	3.850	3.850	3.650	3.850	3.850	3.850	3.850	3.850
$g(r_1)_{i-i}$	0.612	0.708	0.722	0.676	0.717	0.669	0.687	0.691	0.697
$r_{0\ i-j}$	1.750	2.350	2.350	2.250	2.350	1.750	1.750	1.750	1.750
$g(r_0)_{i-j}$	0.001	0.002	0.001	0.001	0.002	0.001	0.001	0.001	0.001
$r_{m\ i-j}$	2.950	2.950	2.950	2.950	2.950	2.950	2.950	2.950	2.950
$g(r_m)_{i-j}$	2.634	2.219	2.149	2.134	2.094	2.426	2.334	2.284	2.246
$r_{1\ i-j}$	3.750	4.150	4.050	4.050	3.850	3.750	3.750	3.750	3.750
$g(r_1)_{i-j}$	0.713	0.667	0.728	0.712	0.770	0.754	0.767	0.777	0.776
$r_{0\ j-j}$	2.450	2.550	2.550	2.550	2.550	2.450	2.450	2.450	2.450
$g(r_0)_{j-j}$	0.003	0.003	0.005	0.004	0.001	0.001	0.001	0.001	0.001
$r_{m\ j-j}$	3.150	3.150	3.150	3.150	3.150	3.150	3.150	3.150	3.150
$g(r_m)_{j-j}$	2.324	2.383	2.319	2.286	2.381	2.354	2.342	2.328	2.339
$r_{1\ j-j}$	4.450	4.450	4.450	4.450	4.550	4.450	4.450	4.450	4.450
$g(r_1)_{j-j}$	0.824	0.838	0.829	0.783	0.866	0.831	0.830	0.818	0.833

Table 3. The three key coordinate points of $g_{In-In}(r)$, $g_{In-Zn}(r)$, and $g_{Zn-Zn}(r)$ in the In50Zn50-730 K system.

Parameters	Step of In50-Zn50 (730 K)									
	0–1000	1000–2000	2000–3000	3000–4000	4000–5000	0–2000	0–3000	0–4000	0–5000	
$r_{0\ i-i}$	2.250	2.550	2.450	2.550	2.550	2.250	2.250	2.250	2.250	
$g(r_{0\ i-i})$	0.003	0.010	0.001	0.011	0.005	0.002	0.001	0.001	0.001	
$r_{m\ i-i}$	3.250	3.150	3.150	3.150	3.150	3.250	3.150	3.150	3.150	
$g(r_{m\ i-i})$	2.368	2.424	2.505	2.429	2.651	2.370	2.397	2.405	2.454	
$r_{1\ i-i}$	4.150	4.250	3.950	4.450	4.250	4.150	4.150	4.150	4.150	
$g(r_{1\ i-i})$	0.777	0.680	0.861	0.680	0.704	0.744	0.757	0.771	0.775	
$r_{0\ i-j}$	2.150	2.350	2.350	2.350	2.350	2.150	2.150	2.150	2.150	
$g(r_{0\ i-j})$	0.001	0.010	0.011	0.004	0.006	0.001	0.001	0.001	0.001	
$r_{m\ i-j}$	2.850	2.850	2.850	2.850	2.850	2.850	2.850	2.850	2.850	
$g(r_{m\ i-j})$	3.045	2.760	2.640	2.654	2.536	2.903	2.815	2.775	2.727	
$r_{1\ i-j}$	3.950	3.950	3.950	3.950	3.950	3.950	3.950	3.950	3.950	
$g(r_{1\ i-j})$	0.695	0.725	0.648	0.630	0.603	0.710	0.689	0.675	0.660	
$r_{0\ j-j}$	2.050	2.050	2.150	2.150	2.150	2.050	2.050	2.050	2.050	
$g(r_{0\ j-j})$	0.001	0.001	0.012	0.009	0.011	0.001	0.001	0.001	0.001	
$r_{m\ j-j}$	2.650	2.550	2.550	2.650	2.550	2.650	2.650	2.650	2.550	
$g(r_{m\ j-j})$	3.455	3.307	3.452	3.353	3.605	3.340	3.371	3.366	3.404	
$r_{1\ j-j}$	3.550	3.650	3.650	3.850	3.550	3.550	3.550	3.650	3.650	
$g(r_{1\ j-j})$	0.455	0.457	0.505	0.574	0.542	0.470	0.486	0.521	0.527	

2.3. Average Pair Potential Energy Functions for Binary Liquid Alloys

The interaction potential function of molecular pairs is an important element in the study of the structure of matter and plays a decisive role in the thermodynamic properties of matter. The unknown parameters in the molar excess Gibbs energy thermodynamic model contain potential energy information. The partial radial distribution function is the result of the dynamic equilibrium of molecules under the action of the potential energy function [33].

According to the equation for the intermolecular pair potential energy as a function of radial distribution in a highly dilute pure gas [34]:

$$g(r) = \exp[-\varepsilon(r)/kT] \quad (1)$$

k is the Boltzmann constant 1.38×10^{-23} J/K and T is the temperature. Assume that this equation can be approximated for i - j binary liquid alloys in order to calculate their interatomic pair potential functions. According to the probability density distribution function and the expectation principle, the expressions for the molecular pair potentials, ε_{ii} , ε_{jj} , and ε_{ij} of the binary liquid alloy can be obtained as [35,36]:

$$\frac{\varepsilon_{ii}}{kT} = \frac{\int_{r_0}^{r_1} \varepsilon_{ii}(r)g_{ii}(r)}{\int_{r_0}^{r_1} 4\pi g_{ii}(r)r^2 dr} dV = -\frac{\int_{r_0}^{r_1} \ln g_{ii}(r)g_{ii}(r)r^2 dr}{\int_{r_0}^{r_1} g_{ii}(r)r^2 dr} \quad (2)$$

$$\frac{\varepsilon_{ij}}{kT} = -\frac{\int_{r_0}^{r_1} \ln g_{ij}(r)g_{ij}(r)r^2 dr}{\int_{r_0}^{r_1} g_{ij}(r)r^2 dr} \quad \frac{\varepsilon_{jj}}{kT} = -\frac{\int_{r_0}^{r_1} \ln g_{jj}(r)g_{jj}(r)r^2 dr}{\int_{r_0}^{r_1} g_{jj}(r)r^2 dr}, \quad (3)$$

Thus, under the condition that $g(r)$ is known, then the values of ε_{ii} , ε_{jj} , and $\varepsilon_{ij} = \varepsilon_{ji}$ can be calculated from Equations (2) and (3).

3. Thermodynamic Model

3.1. Molecular Interaction Volume Model (MIVM)

The MIVM possesses characteristics such as inclusivity, diffusion stability, and thermodynamic consistency. The model satisfies the Gibbs–Duhem equation [37], so it can also be used to describe the thermodynamic properties of partially mutually soluble systems.

Tao used statistical thermodynamics in the derivation process to obtain configurational partition functions that include both volume and energy terms. The model is suitable for different temperature system transformations and has a wide range of applications with relatively mature physical significance.

For the i - j binary alloy system MIVM the molar excess Gibbs energy is expressed as [12]:

$$\frac{G_m^E}{RT} = x_i \ln \left(\frac{V_{mi}}{x_i V_{mi} + x_j V_{mj} B_{ji}} \right) + x_j \ln \left(\frac{V_{mj}}{x_j V_{mj} + x_i V_{mi} B_{ij}} \right) - \frac{x_i x_j}{2} \left[\frac{Z_i B_{ji} \ln B_{ji}}{x_i + x_j B_{ji}} + \frac{Z_j B_{ij} \ln B_{ij}}{x_j + x_i B_{ij}} \right] \quad (4)$$

The molar excess Gibbs energy (G_m^E) measures the overall energy change, and fluid phase equilibrium studies also require knowledge of the component activities (a). The expression for the activity coefficient of component i is [12]:

$$\ln \gamma_i = \ln \left(\frac{V_{mi}}{x_i V_{mi} + x_j V_{mj} B_{ji}} \right) + x_j \left(\frac{V_{mj} B_{ji}}{x_i V_{mi} + x_j V_{mj} B_{ji}} - \frac{V_{mi} B_{ij}}{x_j V_{mj} + x_i V_{mi} B_{ij}} \right) - \frac{x_j^2}{2} \left[\frac{Z_i B_{ji}^2 \ln B_{ji}}{(x_i + x_j B_{ji})^2} + \frac{Z_j B_{ij} \ln B_{ij}}{(x_j + x_i B_{ij})^2} \right] \quad (5)$$

γ_i, γ_j are the activity coefficients of compositions i, j , $a_i = \gamma_i x_i$, $a_j = \gamma_j x_j$ are the respective activities. Where R is the ideal gas constant of 8.314 J/(K.mol). T is the absolute temperature. V_{mi}, V_{mj} denote the molar volume of group elements i, j at the temperature of the system to be solved, respectively. x_i, x_j denote the local mole fractions of the group elements i, j , and Z_i, Z_j denote the first coordination numbers of pure substances i, j . B_{ij} and B_{ji} are the parameters of molecular pair energy interactions, define B_{ij}, B_{ji} [12]:

$$B_{ij} = \exp \left(-\frac{\varepsilon_{ij} - \varepsilon_{jj}}{kT} \right) B_{ji} = \exp \left(-\frac{\varepsilon_{ji} - \varepsilon_{ii}}{kT} \right) \quad (6)$$

3.2. Regular Solution Model (RSM)

The RSM was proposed by Hildebrand in 1929 [6,7]. This model assumes that the mixture enthalpy of the solution is non-zero, while the mixture entropy is equal to that of an ideal solution. In other words, this model considers the interactions between solvent molecules but neglects the influence of volume.

For the i - j binary alloy system RSM the molar excess Gibbs energy is expressed as [6,7]:

$$\frac{G_m^E}{RT} = \frac{w}{kT} x_i x_j \quad (7)$$

The expression for the activity coefficient of component i is [6,7]:

$$\ln \gamma_i = \frac{w}{kT} x_j^2 \quad (8)$$

where w is the interaction parameter. The $\frac{w}{kT}$ expression obtained from Guggenheim's lattice-like theory is used here [38]:

$$\frac{w}{kT} = Z \left[\frac{\varepsilon_{ij}}{kT} - \frac{1}{2} \left(\frac{\varepsilon_{ii}}{kT} + \frac{\varepsilon_{jj}}{kT} \right) \right] \quad (9)$$

Z is the average coordination number. For i - j binary liquid mixtures, the empirical formula for the local coordination number can be replaced by the expression containing the partial radial distribution function given by Hill [34]:

$$\begin{aligned} Z_{ii} &= x_i \rho_0 4\pi \int_0^\infty r^2 g_{ii}(r) dr & Z_{ij} &= x_j \rho_0 4\pi \int_0^\infty r^2 g_{ij}(r) dr \\ Z_{jj} &= x_j \rho_0 4\pi \int_0^\infty r^2 g_{jj}(r) dr & Z_{ji} &= x_i \rho_0 4\pi \int_0^\infty r^2 g_{ji}(r) dr \end{aligned} \quad (10)$$

ρ_0 denotes the corresponding mean density for the corresponding alloy composition. Dorini gives the expression for the average coordination number Z based on the local coordination number of the liquid alloy used here [39]:

$$Z = x_i(Z_{ii} + Z_{ij}) + x_j(Z_{ji} + Z_{jj}) \quad (11)$$

3.3. Wilson Model

The Wilson model was proposed by Wilson in 1964 [8]. Wilson used the ratio of the Boltzmann distribution to define the “local concentration”, in which the local volume fraction was defined. The disadvantage is that it cannot be used in systems where the liquid phase is partially miscible. For the i - j binary alloy system Wilson Model the molar excess Gibbs energy is expressed as [8]:

$$\frac{G_m^E}{RT} = -x_i \ln(x_i + A_{ji}x_j) - x_j \ln(x_j + A_{ij}x_i) \quad (12)$$

The expression for the activity coefficient of component i is [8]:

$$\ln \gamma_i = -\ln(x_i + A_{ji}x_j) + x_j \left[\frac{A_{ji}}{x_i + A_{ji}x_j} - \frac{A_{ij}}{x_j + A_{ij}x_i} \right] \quad (13)$$

where, the parameters A_{ij} and A_{ji} are defined as [8]:

$$A_{ij} = \frac{V_i}{V_j} \exp\left(-\frac{\varepsilon_{ij} - \varepsilon_{jj}}{kT}\right) \quad A_{ji} = \frac{V_j}{V_i} \exp\left(-\frac{\varepsilon_{ij} - \varepsilon_{ii}}{kT}\right) \quad (14)$$

3.4. Non-Random Two-Liquid Model (NRTL)

The NRTL model was proposed by Renon and Prausnitz in 1968 [9]. This model was derived by combining a local composition equation, based on the non-random assumption, with a potential energy expression for liquid mixtures from the two-liquid theory. It overcomes the disadvantage that Wilson’s equation cannot be used for systems in which the liquid phase is partially miscible. This model is often considered the most balanced model in the organic field in terms of simplicity, accuracy, and rationality. Their molar excess Gibbs energy expression [9]:

$$\frac{G_m^E}{RT} = x_i x_j \left(\frac{\tau_{ji} \exp(-\alpha \tau_{ji})}{x_i + x_j \exp(-\alpha \tau_{ji})} + \frac{\tau_{ij} \exp(-\alpha \tau_{ij})}{x_j + x_i \exp(-\alpha \tau_{ij})} \right) \quad (15)$$

The expression for the activity coefficient of component i is [9]:

$$\ln \gamma_i = x_j^2 \left(\frac{\tau_{ji} (\exp(-2\alpha_{ij} \tau_{ji}))^2}{([x_i + x_j \exp(-\alpha_{ij} \tau_{ji})])^2} + \frac{\tau_{ij} \exp(-2\alpha_{ij} \tau_{ij})}{([x_j + x_i \exp(-\alpha_{ij} \tau_{ij})])^2} \right) \quad (16)$$

where, the model parameters τ_{ij} and τ_{ji} are defined as [9]:

$$\tau_{ij} = \frac{\varepsilon_{ij} - \varepsilon_{jj}}{kT} \quad \tau_{ji} = \frac{\varepsilon_{ji} - \varepsilon_{ii}}{kT} \quad (17)$$

The meaning of α is related to the stochasticity of the mixtures, and the value ranges from 0.2 to 0.47, in this paper, we take 0.3; $\alpha_{ij} = \alpha_{ji}$, τ_{ij} , τ_{ji} can be expressed as the pair potential.

3.5. Miedema Model

The Miedema model is a semi-empirical theoretical model developed by Miedema in 1973 [10,11]. This model assumes that the Wigner–Seitz cell theory can be extended from pure metals to binary alloys, and they believe that the concept of cells in alloys is still

valid. The Miedema model generation heat calculation is an important achievement in alloying theory in recent years, with wide practical application. The heat of generation of any binary alloy other than O, S, Se, and Te can be calculated by using the basic properties of the components. The relationship between the partial molar excess free energy \overline{G}_i^E of component i and its activity coefficient in a binary alloy system consisting of component i and component j are expressed as:

$$\overline{G}_i^E = RT \ln \gamma_i \quad (18)$$

The partial molar excess free energy of component i \overline{G}_i^E and the Gibbs excess free energy of the i - j binary alloy system are related by:

$$\overline{G}_i^E = G_{ij}^E + (1 + x_i) \frac{\partial G_{ij}^E}{\partial x_i} \quad (19)$$

In the binary system i - j , the molar excess Gibbs energy G_{ij}^E and excess entropy S_{ij}^E and the enthalpy change of ΔH_{ij} are related by:

$$G_{ij}^E = \Delta H_{ij} - TS_{ij}^E \quad (20)$$

T is the absolute temperature, in binary system alloys, the heat of generation can be obtained from the Miedema model, and the heat of generation in the formation of liquid solution or solid solution is derived as [10,11]:

$$\Delta H_{ij} = f_{ij} \frac{x_i [1 + u_i x_j (\phi_i - \phi_j)] x_j [1 + u_j x_i (\phi_j - \phi_i)]}{x_i V_i^{2/3} [1 + u_i x_j (\phi_i - \phi_j)] + x_j V_j^{2/3} [1 + u_j x_i (\phi_j - \phi_i)]} \quad (21)$$

$$f_{ij} = \frac{2pV_i^{2/3}V_j^{2/3} \left[q/p (n_{wsi}^{1/3} - n_{wsj}^{1/3})^2 - (\phi_i - \phi_j)^2 - a(r/p) \right]}{(n_{ws}^{1/3})_i^{-1} + (n_{ws}^{1/3})_j^{-1}} \quad (22)$$

In Equations (21) and (22), x_i and x_j are the molar fractions of i and j , respectively; V_i and V_j are the molar volumes of group elements i and j , respectively; $(n_{ws})_i$ and $(n_{ws})_j$ are the electron densities of group elements i and j , respectively; ϕ_i and ϕ_j are the electronegativities of group elements i and j ; p , q , μ_i , μ_j , b , r/p are constants and $p/q = 9.4$ for all alloys;

3.5.1. Relationship between Enthalpy of Mixing and Excess Entropy as Defined by Tanaka

Kubaschewski and Alcock [40] examined the relationship between the enthalpy of mixing and excess entropy of binary alloys and concluded that there was an approximately linear relationship. After more careful study, Tanaka concluded that the ratio coefficient of S_{ij}^E and ΔH_{ij} is related to the melting point of pure metals, which can be given by the relation [21]:

$$S_{ij}^E = \frac{\Delta H_{ij} \left[\left(\frac{1}{T_{mi}} \right) + \left(\frac{1}{T_{mj}} \right) \right]}{14} \quad (23)$$

T_{mi} and T_{mj} are monometallic melting points, the same applies below. Order:

$$\beta = 1 - \frac{T \left[\left(\frac{1}{T_{mi}} \right) + \left(\frac{1}{T_{mj}} \right) \right]}{14} \quad (24)$$

Then one can obtain:

$$G_{ij}^E = \beta_{ij} \Delta H_{ij} \quad (25)$$

Combined with the Miedema model Equations (21) and (22), the relationship between the activity coefficients of i as a function of component x_i is obtained:

$$\ln \gamma_i = \frac{1}{RT} \beta_{ij} \Delta H_{ij} \left\{ 1 + x_j \left[\frac{\frac{1}{x_i} - \frac{1}{x_j} - \frac{u_i(\phi_i - \phi_j)}{[1 + u_i x_j(\phi_i - \phi_j)]} + \frac{u_i(\phi_j - \phi_i)}{[1 + u_j x_i(\phi_j - \phi_i)]}}{V_i^{2/3}[1 + u_i(1 - 2x_i)(\phi_i - \phi_j)] + V_j^{2/3}[-1 + u_j(1 - 2x_i)(\phi_j - \phi_i)]} - \frac{x_i V_i^{2/3}[1 + u_i x_j(\phi_i - \phi_j)] + x_j V_j^{2/3}[1 + u_j x_i(\phi_j - \phi_i)]}{} \right] \right\} \quad (26)$$

3.5.2. Relationship between Enthalpy of Mixing and Excess Entropy as Defined by Ding

Ding Xueyong gives different empirical constants based on S_{ij}^E and ΔH_{ij} relationship of [22]:

$$S_{ij}^E = 0.1 \times \Delta H_{ij} [(1/T_{mi}) + (1/T_{mj})] \quad (27)$$

Order:

$$\alpha_{ij} = 1 - 0.1T [(1/T_{mi}) + (1/T_{mj})] \quad (28)$$

Then it is available:

$$G_{ij}^E = \alpha_{ij} \Delta H_{ij} \quad (29)$$

Next, in combined with the Miedema model Equations (21) and (22), the relationship between the activity coefficients of i as a function of component x_i is obtained:

$$\ln \gamma_i = \frac{1}{RT} \alpha_{ij} \Delta H_{ij} \left\{ 1 + x_j \left[\frac{\frac{1}{x_i} - \frac{1}{x_j} - \frac{u_i(\phi_i - \phi_j)}{[1 + u_i x_j(\phi_i - \phi_j)]} + \frac{u_i(\phi_j - \phi_i)}{[1 + u_j x_i(\phi_j - \phi_i)]}}{V_i^{2/3}[1 + u_i(1 - 2x_i)(\phi_i - \phi_j)] + V_j^{2/3}[-1 + u_j(1 - 2x_i)(\phi_j - \phi_i)]} - \frac{x_i V_i^{2/3}[1 + u_i x_j(\phi_i - \phi_j)] + x_j V_j^{2/3}[1 + u_j x_i(\phi_j - \phi_i)]}{} \right] \right\} \quad (30)$$

3.5.3. Relationship between Enthalpy of Mixing and Excess Entropy as Defined by Sommer

For the relationship between the enthalpy of mixing and excess entropy, Sommer, Germany, gave the following new expression based on the formula of V.T. Witusiewicz [41] in combination with binary system alloys [23,24]:

$$S_{ij}^E = \Omega \left[\frac{\Delta H}{T} + x_i x_j R P_T \right] \quad (31)$$

Among them [23,24]:

$$\Omega = \frac{1}{2\pi} \left(\frac{\bar{T}_m}{\bar{T}_b} + 1 \right) \quad (32)$$

$$P_T = \frac{1}{2} + \frac{4\bar{T}_m}{3T} + 2 \ln \frac{T}{\bar{T}_b - \bar{T}_m} \quad (33)$$

T_{bi} and T_{bj} are monometallic boiling points, respectively. $\bar{T}_m = (T_{mi} + T_{mj})/2$; $\bar{T}_b = (T_{bi} + T_{bj})/2$, e is a natural constant.

Combining Equations (18), (19) and (29), $\ln \gamma_i$ can be expressed as:

$$\ln \gamma_i = \frac{\alpha_{ij} H_{ij}}{RT} + \frac{\alpha_{ij}(1 + x_i) \frac{\partial \Delta H_{ij}}{\partial x_i}}{RT} \quad (34)$$

Associative formulations (30) and (34) are available for the Miedema model:

$$\frac{\partial \Delta H_{ij}}{\partial x_i} = \Delta H_{ij} \left(\frac{1 - x_i}{1 + x_i} \right) \left[\frac{\frac{1}{x_i} - \frac{1}{1 - x_i} - \frac{\mu_i(\phi_i - \phi_j)}{[1 + \mu_i(1 - x_i)(\phi_i - \phi_j)]} + \frac{\mu_i(\phi_j - \phi_i)}{[1 + \mu_j x_i(\phi_j - \phi_i)]}}{V_i^{2/3}[1 + \mu_i(1 - 2x_i)(\phi_i - \phi_j)] + V_j^{2/3}[-1 + \mu_j(1 - 2x_i)(\phi_j - \phi_i)]} - \frac{x_i V_i^{2/3}[1 + \mu_i x_j(\phi_i - \phi_j)] + x_j V_j^{2/3}[1 + \mu_j x_i(\phi_j - \phi_i)]}{} \right] \quad (35)$$

The Sommer enthalpy change and entropy change relation combining Equations (18)–(20), (31)–(33) and (35) can ultimately lead to the derivation of expressions for the molar excess Gibbs energy and activity:

$$G_{ij}^E = (1 - \Omega) \Delta H_{ij} - x_i(1 - x_i) T \Omega R P_T \quad (36)$$

$$\ln \gamma_i = \frac{(1-\Omega)\Delta H_{ij} - x_i(1-x_i)T\Omega RP_T}{RT} + \frac{(1+x_i)\left[(1-\Omega)\frac{\partial \Delta H_{ij}}{\partial x_i} - (1-2x_i)T\Omega RP_T\right]}{RT}$$

$$= \frac{(1-\Omega)\Delta H_{ij} - x_i(1-x_i)T\Omega RP_T}{RT} + \frac{(1-x_i)(1-\Omega)\Delta H_{ij}}{RT} \left[\frac{1}{x_i} - \frac{1}{1-x_i} - \frac{\mu_i(\varphi_i - \varphi_j)}{[1 + \mu_i(1-x_i)(\varphi_i - \varphi_j)]} + \frac{\mu_i(\varphi_j - \varphi_i)}{[1 + \mu_j x_i(\varphi_j - \varphi_i)]} \right] - (1+x_i)(1-2x_i)T\Omega RP_T$$

$$+ \frac{-\frac{V_i^{2/3}[1 + \mu_i(1-2x_i)(\varphi_i - \varphi_j)] + V_j^{2/3}[-1 + \mu_j(1-2x_i)(\varphi_j - \varphi_i)]}{x_i V_i^{2/3}[1 + \mu_i x_j(\varphi_i - \varphi_j)] + x_j V_j^{2/3}[1 + \mu_j x_i(\varphi_j - \varphi_i)]}}{RT}$$
(37)

For the Miedema model parameters are shown in Table 4. where the r/p value is only relevant for transition metal and non-transition metal alloys, and for two non-transition metals the p value is 10.6.

Table 4. Parameters for Miedema model calculation of Pb-Sn, Al-Sn, In-Zn systems [42].

Metal	Φ	$n_{ws}^{1/3}$	$V^{2/3}$	μ	α	T_m/K	T_b/K	r/p
Pb	4.1	1.15	6.9	0.04	0.73	1050	2022	2.1
Al	4.2	1.39	4.6	0.07	0.73	933	2793	1.9
Sn	4.15	1.24	6.4	0.04	0.73	505	2875	2.1
In	3.9	1.17	6.3	0.07	0.73	430	2345	1.9
Zn	4.1	1.32	4.4	0.1	0.73	693	1181	1.4

4. Results and Discussion

4.1. Parameters of Four Models

The expressions (2) and (3) for the average atom pair potential of the binary liquid alloy containing $g(r)$ are substituted into the model parameter expressions (6), (9), (14), and (17) for MIVM, RSM, Wilson, and NRTL, respectively, and the values of the integral terms are calculated by using the graphical integration method with trapezoidal integration as the basic principle [43]. This method divides the integration region into several small trapezoids and sums their areas to obtain the integral value. Obviously, this method is different from the mathematical form of L-PPDF fitted with the Gaussian function by Chunlong Wang et al. [31], which depends on the fitting parameters u and v . Therefore, in this work, no fitting parameters are introduced in the process of solving each model parameter.

The parameter values of each model are calculated by using the asymmetric method and the symmetric method, as shown in Table 5. For the parameters of the symmetry method, the table presents the data calculated by multiplying by two the integral values of $r_0 \sim r_m$ in the selected $g(r)$.

In order to visualize the difference between the fitted values and the experimental values more intuitive, the standard deviation SD and the average relative deviation ARD of the calculated results are denoted as:

$$SD = \sqrt{\frac{\sum (a_{est} - a_{exp})^2}{N}}, \quad ARD = \frac{1}{N} \sum \left| \frac{a_{est} - a_{exp}}{a_{exp}} \right| \times 100\%$$

a_{est} is the estimated value of activity and a_{exp} [43–45] is the experimental value of activity.

$$SD = \sqrt{\frac{\sum (G_m^E(est) - G_m^E(exp))^2}{N}}, \quad ARD = \frac{1}{N} \sum \left| \frac{G_m^E(est) - G_m^E(exp)}{G_m^E(exp)} \right| \times 100\%$$

$G_m^E(est)$ is the estimated value of the molar excess Gibbs energy and $G_m^E(exp)$ [44–46] is the experimental value of the molar excess Gibbs energy.

Table 5. Parameters of four models were calculated for Pb-Sn, Al-Sn, and In-Zn systems by asymmetric and symmetric methods.

System	Step	MIVM				RSM		Wilson				NRTL			
		Asym		Sym		Asym	Sym	Asym		Sym		Asym		Sym	
		B_{ij}	B_{ji}	B_{ij}	B_{ji}	w/kT	w/kT	A_{ij}	A_{ji}	A_{ij}	A_{ji}	τ_{ij}	τ_{ji}	τ_{ij}	τ_{ji}
Pb50-Sn50 (1050 K)	0–1000	0.87	0.97	0.98	0.94	1.08	0.25	0.85	1.00	0.83	1.12	0.03	0.14	0.06	0.02
	1000–2000	0.84	0.96	1.01	0.98	1.49	0.04	0.84	0.96	0.86	1.16	0.05	0.18	0.02	−0.01
	2000–3000	0.94	1.09	0.96	1.02	0.14	0.06	0.95	1.08	0.90	1.09	−0.08	0.06	−0.02	0.04
	3000–4000	1.09	0.98	0.92	1.02	0.37	0.15	0.86	1.24	0.90	1.05	0.02	−0.08	−0.02	0.09
	4000–5000	0.94	1.05	1.01	0.98	0.09	0.05	0.92	1.08	0.86	1.15	−0.05	0.06	0.02	−0.01
	0–2000	0.95	0.98	0.95	1.02	0.51	0.11	0.85	1.08	0.89	1.09	0.03	0.05	−0.02	0.05
	0–3000	0.87	1.00	0.96	1.02	0.86	0.09	0.88	1.00	0.89	1.09	0.00	0.13	−0.02	0.05
	0–4000	0.99	1.00	0.95	1.02	0.11	0.10	0.87	1.13	0.89	1.08	0.01	0.01	−0.02	0.06
	0–5000	0.98	0.99	0.94	1.01	0.18	0.16	0.87	1.12	0.89	1.07	0.01	0.02	−0.01	0.07
Al50-Sn50 (973 K)	0–1000	1.14	0.79	1.18	0.70	0.54	0.50	1.19	0.76	1.06	0.78	0.24	−0.13	0.36	−0.17
	1000–2000	0.89	0.64	0.98	0.64	3.50	1.18	0.97	0.59	0.96	0.65	0.44	0.12	0.45	0.02
	2000–3000	0.90	0.68	0.93	0.60	3.01	1.48	1.02	0.60	0.90	0.62	0.39	0.10	0.51	0.07
	3000–4000	0.88	0.59	0.95	0.59	3.93	1.46	0.89	0.58	0.89	0.63	0.53	0.13	0.53	0.05
	4000–5000	0.93	0.66	0.89	0.56	2.90	1.76	0.99	0.62	0.85	0.59	0.42	0.07	0.58	0.12
	0–2000	1.08	0.79	1.08	0.67	0.89	0.83	1.18	0.72	1.01	0.72	0.24	−0.08	0.40	−0.08
	0–3000	1.05	0.78	1.03	0.65	1.11	1.05	1.17	0.70	0.98	0.68	0.26	−0.05	0.43	−0.03
	0–4000	1.03	0.76	1.01	0.63	1.32	1.15	1.15	0.69	0.95	0.67	0.27	−0.03	0.46	−0.01
	0–5000	1.01	0.75	0.98	0.62	1.55	1.27	1.12	0.67	0.93	0.65	0.29	−0.01	0.48	0.02
In50-Zn50 (730 K)	0–1000	0.95	1.08	0.81	1.22	0.17	0.24	0.66	1.56	0.74	1.33	−0.08	0.05	−0.20	0.21
	1000–2000	0.93	1.05	0.86	1.14	0.16	0.00	0.64	1.53	0.69	1.41	−0.05	0.07	−0.13	0.15
	2000–3000	0.85	0.89	0.79	1.04	1.61	0.42	0.54	1.39	0.64	1.29	0.12	0.16	−0.04	0.24
	3000–4000	0.93	1.06	0.73	1.04	0.09	0.94	0.65	1.52	0.63	1.20	−0.06	0.08	−0.04	0.32
	4000–5000	0.76	0.96	0.74	0.96	1.88	0.78	0.58	1.25	0.58	1.22	0.05	0.27	0.04	0.30
	0–2000	0.92	1.04	0.79	1.13	0.24	0.58	0.64	1.51	0.69	1.30	−0.04	0.09	−0.13	0.23
	0–3000	0.88	1.01	0.76	1.17	0.66	0.47	0.62	1.44	0.71	1.25	−0.01	0.13	−0.16	0.28
	0–4000	0.91	1.00	0.75	1.14	0.58	0.59	0.61	1.49	0.69	1.23	0.00	0.10	−0.13	0.29
	0–5000	0.88	0.98	0.83	1.10	0.82	0.16	0.60	1.45	0.67	1.36	0.02	0.12	−0.09	0.18

4.2. Miedema Model Estimation of Molar Excess Gibbs Energy and Activity

The Miedema model is an empirical theoretical model. The molar excess Gibbs energy and activity of a binary alloy system can be estimated by the Miedema formula in combination with the basic properties of the group elements and the relevant parameters, simply by knowing the equation of the corresponding enthalpy of mixing of the alloy system in relation to the excess entropy. The experimental values of full concentration molar excess Gibbs energy (G_m^E), activity (a) of Pb-Sn, Al-Sn, and In-Zn alloys under the Miedema model are given below with the comparison and deviation of the calculated values in Tables 6–8 and Figures 5–7.

Table 6. Comparison of experimental and calculated values of molar excess Gibbs energy and activity for Pb-Sn alloys all at full concentration in the Miedema model at 1050 K.

Molar Excess Gibbs Energy (J/mol)				
x_i	Exp	Ding	Tanaka	Sommer
0.9	436	334	393	387
0.8	801	598	704	693
0.7	1085	791	931	916
0.6	1279	910	1071	1054
0.5	1373	955	1124	1106
0.4	1356	923	1087	1069
0.3	1221	814	958	942
0.2	956	624	735	723
0.1	552	354	416	410
ARD%		30.11%	17.73%	19.05%
SD		325	197	210

Table 6. Cont.

x_i	Activity							
	a_i -Exp	a_j -Exp	a_i -Ding	a_j -Ding	a_i -Tanaka	a_j -Tanaka	a_i -Sommer	a_j -Sommer
0.9	0.904	0.159	0.904	0.141	0.904	0.150	0.904	0.149
0.8	0.814	0.296	0.813	0.264	0.815	0.277	0.815	0.276
0.7	0.730	0.412	0.726	0.372	0.731	0.387	0.731	0.385
0.6	0.650	0.512	0.641	0.470	0.649	0.483	0.648	0.482
0.5	0.572	0.599	0.556	0.560	0.566	0.571	0.565	0.570
0.4	0.492	0.677	0.467	0.646	0.480	0.654	0.478	0.653
0.3	0.405	0.752	0.371	0.730	0.385	0.735	0.384	0.735
0.2	0.303	0.827	0.265	0.815	0.279	0.818	0.277	0.818
0.1	0.174	0.908	0.144	0.904	0.153	0.905	0.152	0.905
ARD% of Single Component			5.37%	6.18%	3.22%	3.89%	3.43%	4.13%
SD of Single Component			0.022	0.029	0.013	0.02	0.014	0.021
ARD%			5.77%		3.55%		3.78%	
SD			0.026		0.017		0.018	

Table 7. Comparison of experimental and calculated values of molar excess Gibbs energy and activity for Al-Sn alloys all at full concentration in the Miedema model at 973 K.

x_i	Molar Excess Gibbs Energy (J/mol)							
	Exp	Ding		Tanaka		Sommer		
0.9	1318	1130		1266		1149		
0.8	2194	1937		2171		1970		
0.7	2703	2454		2750		2498		
0.6	2911	2711		3039		2761		
0.5	2870	2733		3063		2784		
0.4	2624	2542		2849		2591		
0.3	2200	2158		2418		2200		
0.2	1619	1596		1788		1628		
0.1	887	872		977		890		
ARD%		6.11%		6.34%		4.55%		
SD		160		147		130		
x_i	Activity							
	a_i -Exp	a_j -Exp	a_i -Ding	a_j -Ding	a_i -Tanaka	a_j -Tanaka	a_i -Sommer	a_j -Sommer
0.9	0.927	0.393	0.919	0.335	0.921	0.388	0.919	0.343
0.8	0.887	0.514	0.864	0.487	0.872	0.542	0.865	0.495
0.7	0.859	0.567	0.823	0.566	0.839	0.611	0.825	0.573
0.6	0.828	0.606	0.784	0.618	0.810	0.652	0.788	0.624
0.5	0.782	0.650	0.740	0.664	0.776	0.687	0.745	0.668
0.4	0.711	0.702	0.680	0.711	0.725	0.726	0.686	0.714
0.3	0.609	0.762	0.591	0.766	0.642	0.774	0.599	0.768
0.2	0.468	0.831	0.461	0.831	0.510	0.835	0.468	0.832
0.1	0.274	0.909	0.271	0.908	0.306	0.909	0.277	0.908
ARD% of Single Component			3.12%	2.93%	3.94%	3.68%	2.58%	2.89%
SD of Single Component			0.028	0.022	0.024	0.028	0.025	0.021
ARD%			3.03%		3.81%		2.74%	
SD			0.025		0.026		0.023	

Table 8. Comparison of experimental and calculated values of molar excess Gibbs energy and activity for In-Zn alloys all at full concentration in the Miedema model at 730 K.

Molar Excess Gibbs Energy (J/mol)				
x_i	Exp	Ding	Tanaka	Sommer
0.9	726	679	752	523
0.8	1321	1241	1375	961
0.7	1785	1677	1859	1305
0.6	2112	1975	2190	1546
0.5	2288	2124	2354	1670
0.4	2295	2107	2335	1666
0.3	2105	1907	2114	1516
0.2	1686	1506	1669	1203
0.1	1000	879	974	706
	ARD%	8.08%	2.68%	27.71%
	SD	144	50	491

Activity								
x_i	a_i -Exp	a_j -Exp	a_i -Ding	a_j -Ding	a_i -Tanaka	a_j -Tanaka	a_i -Sommer	a_j -Sommer
0.9	0.910	0.300	0.908	0.281	0.909	0.315	0.906	0.223
0.8	0.835	0.500	0.832	0.475	0.836	0.522	0.823	0.393
0.7	0.772	0.636	0.769	0.606	0.777	0.653	0.750	0.522
0.6	0.719	0.728	0.716	0.692	0.730	0.735	0.685	0.619
0.5	0.674	0.788	0.671	0.750	0.692	0.784	0.625	0.693
0.4	0.636	0.827	0.628	0.792	0.659	0.816	0.567	0.752
0.3	0.598	0.854	0.578	0.828	0.621	0.843	0.501	0.803
0.2	0.542	0.882	0.502	0.867	0.555	0.874	0.414	0.855
0.1	0.407	0.925	0.350	0.920	0.401	0.922	0.272	0.916
	ARD% of Single Component		3.07%	3.93%	1.81%	1.91%	11.16%	12.34%
	SD of Single Component		0.024	0.027	0.014	0.012	0.077	0.082
	ARD%		3.50%		1.86%		11.75%	
	SD		0.026		0.013		0.079	

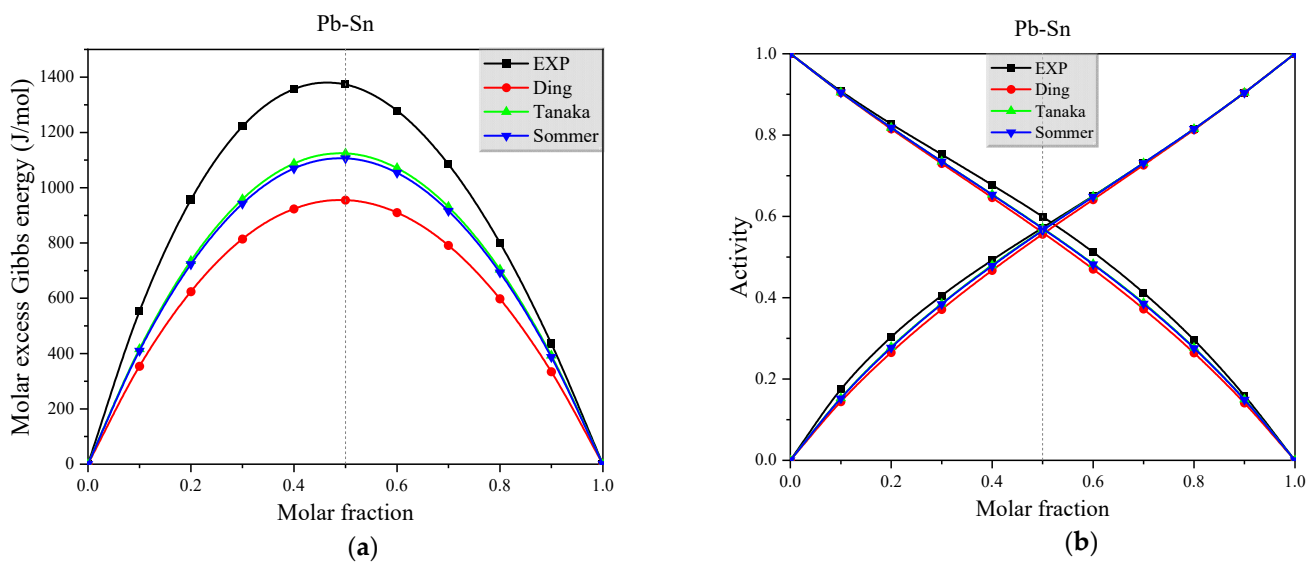


Figure 5. (a) The experimental and calculated values of molar excess Gibbs energy for the full concentration of Pb-Sn alloys in the Miedema model at 1050 K, (b) The experimental and calculated values of activity for the full concentration of Pb-Sn alloys in the Miedema model at 1050 K.

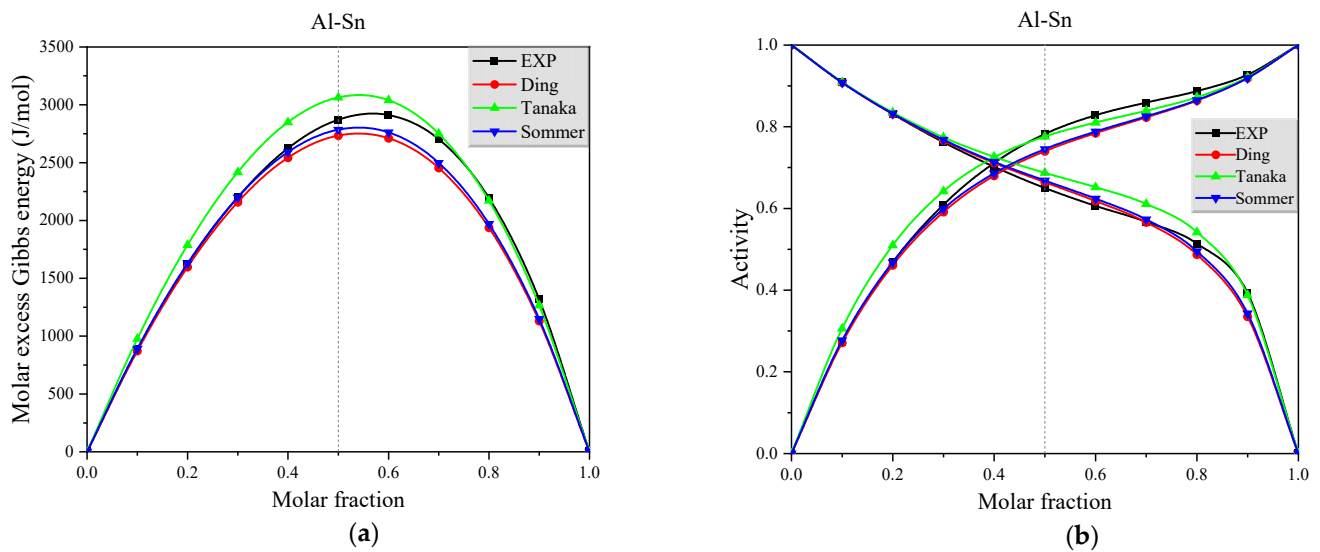


Figure 6. (a) The experimental and calculated values of molar excess Gibbs energy for the full concentration of Al-Sn alloys in the Miedema model at 973 K, (b) The experimental and calculated values of activity for the full concentration of Al-Sn alloys in the Miedema model at 973 K.

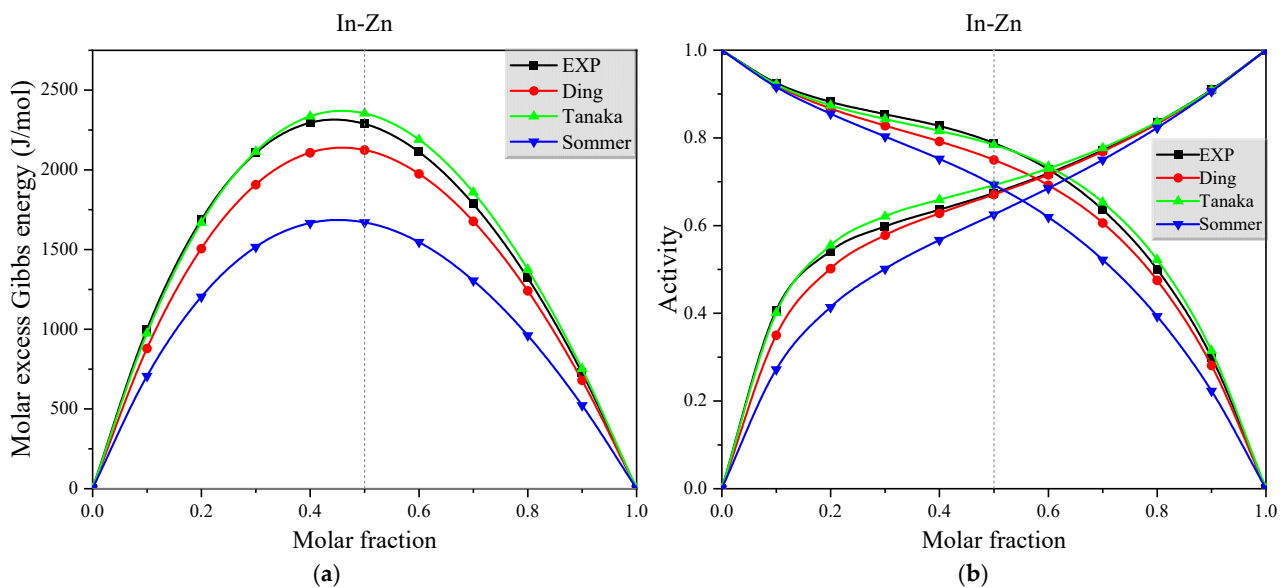


Figure 7. (a) The experimental and calculated values of molar excess Gibbs energy for the full concentration of In-Zn alloys in the Miedema model at 730 K, (b) The experimental and calculated values of activity for the full concentration of In-Zn alloys in the Miedema model at 730 K.

Figure 5 and Table 6 show that for Pb-Sn alloys Tanaka Ding, and Sommer's improved mixing enthalpy versus excess entropy relationship equation in the Miedema model to estimate the activity effect ARD is less than 10%. However, since the experimental values of the activity of Pb-Sn alloys are consistent with symmetry and are the effect of the presentation of very small deviations, so there is a possibility of chance in the estimation results.

Figure 6 and Table 7 show that the estimation effect of the three methods for Al-Sn alloys is obvious. The activity ARD of the three methods is less than 5%, and the ARD of the estimated molar excess Gibbs energy is less than 10%, the estimation effect can be said to be accurate. The Sommer's improved mixing enthalpy versus excess entropy relationship equation in the Miedema model has a better estimation effect.

Figure 7 and Table 8 show that for In-Zn alloys, Sommer's formula is slightly less effective than the first two in estimating activity, with an ARD of 11.75%, while the ARD

of the other two is less than 5%. This shows that all three methods give relatively good estimation results for different systems. The relation between the enthalpy of mixing and excess entropy given by Sommer is based on the application of the Miedema model to binary alloys in order to estimate the activity and molar excess Gibbs energy is reasonable and feasible. The total average relative deviations of Tanaka, Ding, and Sommer's relational equations in the Miedema model for estimating the activities and molar excess Gibbs energies of the binary liquid alloys Pb-Sn, Al-Sn, and In-Zn are 3.07% and 8.92%, 6.09% and 17.1%, and 4.1% and 14.77%, respectively.

4.3. Estimation of the Molar Excess Gibbs Energy and Activity of $Pb_{0.5}Sn_{0.5}$, $Al_{0.5}Sn_{0.5}$, and $In_{0.5}Zn_{0.5}$ Alloys at Full Concentration Using Partial Radial Distribution Functions

Tables 9–14 show the results of stepwise calculations for the three systems using the symmetric and asymmetric methods in the four models, respectively. The ARD comparison images of all the activity distributions calculated for the three binary alloy systems under the asymmetric and symmetric methods are given, where the x-axis represents the four models. The two small bars for each model represent the asymmetric and symmetric methods under each model, the different colors of each bar represent the different ranges of the ARD values, and the scale of the bar is the number of data accounted for by the calculations of the nine sets of distributions, see Figures 8–10.

Through Figure 8 it can be seen that the MIVM model in Pb-Sn alloy has the best overall estimation effect. The ARD less than 10% accounts for five of the nine sets of stepwise calculation data under the two methods. The symmetric method under the MIVM model has a better estimation performance. The RSM model has the second-best estimation performance, and the asymmetric method under the RSM model has a better estimation effect. The estimation effect of the Wilson and the NRTL models is poorer compared with the former two, there is no data of ARD less than 10%.

Through Figure 9 it can be seen in Al-Sn alloys in the RSM model the two methods ARD less than 20% of the data in the two methods under the nine groups of stepwise calculation data accounted for eight groups. Among the asymmetric methods, there were two groups with ARDs less than 10% and four groups with ARDs greater than 30%. The Figure 9 can only show that for the RSM model for Al-Sn alloys, the asymmetric method estimation of the precision of the higher degree of data is greater. The data with a high estimation degree of the MIVM model is second only to the RSM model and the asymmetric method is better under the MIVM model. Wilson model and NRTL model estimation of activity ARD has no data less than 20%, but there is more data with ARD between 20–30%, so it is necessary to calculate the average value to compare the estimation effect.

Figure 10 shows that the overall estimation effect of the MIVM model in In-Zn alloys is better. The ARD less than 30% accounts for seven of the nine sets of stepwise calculation data in the two methods, in which the symmetric method has a better estimation effect. The estimation effect of the RSM model is second to that of the MIVM model, in which the asymmetric method has a better estimation effect. The estimation effect of the Wilson model and the NRTL model is poorer compared to the former two, and the ARD does not have any data of less than 30%.

According to the data in Tables 9–14, it can be calculated that the total average relative deviations of the activity estimates of the four models for the binary liquid alloys $Pb_{50}Sn_{50}$, $Al_{50}Sn_{50}$, and $In_{50}Zn_{50}$ at the full concentrations. When the PRDF is obtained by the symmetry method are MIVM: 21.59%; RSM: 21.63%; Wilson: 24.27%; and NRTL: 23.9%. When the PRDF is obtained by the symmetry method are MIVM: 22.86%; RSM: 32.84%; Wilson: 25.14%; NRTL: 24.49%. Combined with Figures 8–10, it can be concluded that the symmetric method of estimation is better than the asymmetric method in the three binary alloy systems. Among the four models, the MIVM model has a better estimation effect. The estimation results of the MIVM and RSM models fluctuate greatly with the number of steps, and the data distribution is not uniform. However, because of the high sensitivity of the estimation effect to the change in the number of steps, the estimation results are

more consistent with the experimental values. The Wilson and NRTL models estimate the activity data with less variation as the number of steps changes, and the estimation effect is not good. The data obtained from Tables 9–14 also reflect that not all systems are best estimated at 0–5000 steps (at full steps size).

Table 9. The SD and ARD of molar excess Gibbs energy and activity of Pb50Sn50 alloys were estimated by asymmetric method at 1050 K.

G_m^E and a	Step	MIVM		RSM		Wilson		NRTL	
		ARD%	SD	ARD%	SD	ARD%	SD	ARD%	SD
G_m^E (J/mol)	0~1000	61.4%	642	72.4%	760	74.2%	787	73.7%	782
	1000~2000	107.9%	1131	137.0%	1441	66.2%	704	65.9%	701
	2000~3000	131.5%	1390	121.8%	1288	104.0%	1100	103.3%	1093
	3000~4000	166.8%	1758	159.8%	1685	112.5%	1190	109.8%	1161
	4000~5000	91.2%	965	86.0%	911	98.3%	1040	97.7%	1034
	0~2000	25.4%	265	37.0%	388	79.4%	939	87.6%	928
	0~3000	22.7%	250	18.1%	199	88.7%	842	79.2%	839
	0~4000	85.1%	902	82.6%	876	98.8%	1045	97.4%	1031
	0~5000	74.7%	793	71.6%	760	97.1%	1027	95.8%	1014
	Average	85.2%	899	87.4%	923	91.0%	964	90.0%	954
a	0~1000	13.4%	0.057	16.2%	0.069	13.1%	0.058	13.0%	0.057
	1000~2000	25.8%	0.108	34.8%	0.144	11.9%	0.052	11.8%	0.052
	2000~3000	21.2%	0.094	20.0%	0.088	17.5%	0.077	17.5%	0.077
	3000~4000	25.6%	0.114	24.7%	0.11	18.7%	0.083	18.4%	0.081
	4000~5000	15.7%	0.069	14.9%	0.066	16.7%	0.074	16.7%	0.074
	0~2000	5.2%	0.022	7.8%	0.034	15.3%	0.068	15.1%	0.067
	0~3000	4.5%	0.021	3.7%	0.017	13.9%	0.061	13.9%	0.061
	0~4000	14.8%	0.065	14.4%	0.064	16.8%	0.074	16.6%	0.073
	0~5000	13.2%	0.058	12.7%	0.056	16.5%	0.073	16.4%	0.072
	Average	15.5%	0.068	16.6%	0.072	15.6%	0.069	15.5%	0.068

Table 10. The SD and ARD of molar excess Gibbs energy and activity of Pb50Sn50 alloys were estimated by symmetric method at 1050 K.

G_m^E and a	Step	MIVM		RSM		Wilson		NRTL	
		ARD%	SD	ARD%	SD	ARD%	SD	ARD%	SD
G_m^E (J/mol)	0~1000	14.2%	171	59.7%	632	88.7%	939	85.9%	911
	1000~2000	117.3%	1239	106.0%	1122	104.6%	1106	102.4%	1083
	2000~3000	83.3%	883	90.8%	962	97.5%	1032	96.8%	1024
	3000~4000	53.1%	565	76.7%	813	92.1%	976	91.7%	971
	4000~5000	123.7%	1306	108.5%	1148	105.7%	1118	103.3%	1092
	0~2000	62.3%	662	82.5%	874	94.3%	998	93.5%	990
	0~3000	71.7%	761	86.2%	914	95.8%	1014	95.0%	1006
	0~4000	66.8%	710	83.9%	889	94.9%	1004	94.2%	997
	0~5000	45.3%	483	74.3%	788	91.5%	969	90.8%	962
	Average	70.8%	753	85.4%	905	96.1%	1017	94.8%	1004
a	0~1000	3.2%	0.016	13.7%	0.06	15.3%	0.068	15.0%	0.066
	1000~2000	19.4%	0.086	17.4%	0.077	17.6%	0.078	17.3%	0.076
	2000~3000	14.5%	0.064	16.3%	0.072	16.6%	0.073	16.5%	0.073
	3000~4000	9.7%	0.043	15.2%	0.067	15.8%	0.07	15.8%	0.07
	4000~5000	20.2%	0.09	17.5%	0.077	17.8%	0.079	17.4%	0.077
	0~2000	11.2%	0.049	15.7%	0.069	16.1%	0.071	16.0%	0.071
	0~3000	12.7%	0.056	16.0%	0.07	16.3%	0.072	16.3%	0.072
	0~4000	12.0%	0.053	15.8%	0.07	16.2%	0.072	16.1%	0.071
	0~5000	8.4%	0.037	15.0%	0.066	15.7%	0.069	15.6%	0.069
	Average	12.4%	0.055	15.8%	0.07	16.4%	0.072	16.2%	0.072

Table 11. The SD and ARD of molar excess Gibbs energy and activity of Al50Sn50 alloys were estimated by asymmetric method at 973 K.

G_m^E and a	Step	MIVM		RSM		Wilson		NRTL		
		ARD%	SD	ARD%	SD	ARD%	SD	ARD%	SD	
G_m^E (J/mol)	0~1000	60.4%	1359	43.6%	986	94.9%	2139	92.0%	2075	
	1000~2000	71.1%	1600	100.0%	2242	65.5%	1481	60.0%	1361	
	2000~3000	56.5%	1270	76.4%	1715	69.8%	1577	64.7%	1467	
	3000~4000	89.5%	2017	120.7%	2716	59.1%	1338	52.6%	1197	
	4000~5000	51.1%	1154	70.5%	1587	69.7%	1574	64.6%	1464	
	0~2000	55.6%	1249	38.5%	881	91.3%	2057	88.0%	1985	
	0~3000	38.1%	858	23.3%	550	88.8%	2001	85.3%	1925	
	0~4000	22.4%	506	9.1%	253	86.3%	1946	82.6%	1866	
	0~5000	6.0%	148	10.5%	227	83.6%	1885	79.7%	1801	
	Average	50.1%	1129	54.7%	1240	78.8%	1778	74.4%	1682	
	a	0~1000	20.2%	0.132	15.7%	0.104	30.9%	0.202	30.7%	0.201
		1000~2000	50.8%	0.33	88.8%	0.565	23.2%	0.156	22.6%	0.15
		2000~3000	36.6%	0.236	57.4%	0.365	24.5%	0.164	23.8%	0.157
3000~4000		72.9%	0.483	126.6%	0.809	21.4%	0.145	20.9%	0.139	
4000~5000		32.1%	0.209	51.1%	0.325	24.4%	0.163	24.0%	0.158	
0~2000		20.4%	0.134	14.8%	0.104	30.0%	0.197	29.7%	0.194	
0~3000		14.8%	0.098	9.9%	0.074	29.4%	0.193	29.0%	0.19	
0~4000		9.1%	0.061	6.6%	0.051	28.8%	0.19	28.4%	0.186	
0~5000		2.8%	0.022	8.3%	0.054	28.1%	0.186	27.7%	0.182	
Average		28.8%	0.256	58.3%	0.376	26.7%	0.177	26.3%	0.173	

Table 12. The SD and ARD of molar excess Gibbs energy and activity of Al50Sn50 alloys were estimated by symmetric method at 973 K.

G_m^E and a	Step	MIVM		RSM		Wilson		NRTL		
		ARD%	SD	ARD%	SD	ARD%	SD	ARD%	SD	
G_m^E (J/mol)	0~1000	45.1%	1008	65.2%	1484	87.9%	1982	84.5%	1906	
	1000~2000	37.9%	862	17.8%	466	71.1%	1606	66.0%	1495	
	2000~3000	67.9%	1536	12.3%	236	63.6%	1439	57.6%	1308	
	3000~4000	63.0%	1428	12.2%	233	63.7%	1443	57.6%	1307	
	4000~5000	106.1%	2095	23.4%	546	56.9%	1290	49.9%	1136	
	0~2000	4.4%	87	41.8%	970	79.5%	1795	75.4%	1703	
	0~3000	29.8%	685	27.1%	655	74.3%	1678	69.6%	1574	
	0~4000	44.9%	1026	19.9%	508	71.7%	1620	66.6%	1508	
	0~5000	63.1%	1435	12.9%	349	68.7%	1553	63.3%	1434	
	Average	51.4%	1129	25.8%	605	70.8%	1601	65.6%	1486	
	a	0~1000	16.2%	0.104	27.8%	0.183	29.2%	0.192	29.4%	0.192
		1000~2000	22.0%	0.145	20.4%	0.137	24.8%	0.165	24.6%	0.162
		2000~3000	47.7%	0.315	16.1%	0.112	22.7%	0.153	22.4%	0.148
3000~4000		42.9%	0.285	16.5%	0.114	22.8%	0.153	22.6%	0.149	
4000~5000		77.8%	0.521	12.1%	0.089	20.7%	0.141	20.3%	0.135	
0~2000		1.6%	0.01	24.4%	0.162	27.1%	0.179	27.1%	0.178	
0~3000		15.8%	0.105	22.0%	0.147	25.7%	0.171	25.6%	0.169	
0~4000		25.2%	0.167	20.7%	0.139	25.0%	0.166	24.9%	0.164	
0~5000		38.1%	0.252	19.2%	0.13	24.2%	0.161	24.0%	0.158	
Average		31.9%	0.212	19.9%	0.135	24.7%	0.165	24.6%	0.162	

Table 13. The SD and ARD of molar excess Gibbs energy and activity of In50Zn50 alloys were estimated by asymmetric method at 730 K.

G_m^E and a	Step	MIVM		RSM		Wilson		NRTL		
		ARD%	SD	ARD%	SD	ARD%	SD	ARD%	SD	
G_m^E (J/mol)	0~1000	123.0%	2197	111.2%	1986	108.0%	1929	101.8%	1818	
	1000~2000	98.4%	1757	89.5%	1598	104.4%	1865	98.2%	1753	
	2000~3000	8.4%	140	8.4%	143	89.2%	1591	81.8%	1463	
	3000~4000	103.8%	1855	93.8%	1675	105.0%	1874	98.9%	1767	
	4000~5000	12.5%	230	22.9%	420	84.7%	1511	80.1%	1432	
	0~2000	92.2%	1647	84.0%	1500	103.3%	1844	97.2%	1736	
	0~3000	63.2%	1131	57.1%	1019	98.5%	1758	92.7%	1655	
	0~4000	67.9%	1215	62.0%	1108	100.0%	1785	93.6%	1671	
	0~5000	51.3%	921	46.1%	826	97.2%	1735	90.9%	1625	
	Average	69.0%	1233	63.9%	1142	98.9%	1766	92.8%	1658	
	a	0~1000	38.2%	0.259	34.6%	0.234	35.2%	0.238	33.9%	0.229
		1000~2000	33.0%	0.224	32.2%	0.218	34.4%	0.233	33.0%	0.223
		2000~3000	5.3%	0.036	6.9%	0.046	30.8%	0.21	28.9%	0.196
3000~4000		34.2%	0.232	31.9%	0.216	34.5%	0.233	33.2%	0.225	
4000~5000		6.8%	0.047	13.9%	0.096	29.6%	0.202	28.4%	0.193	
0~2000		31.6%	0.214	29.5%	0.2	34.1%	0.231	32.8%	0.222	
0~3000		23.8%	0.162	21.8%	0.15	33.0%	0.224	31.7%	0.215	
0~4000		25.2%	0.171	23.4%	0.16	33.4%	0.226	31.9%	0.216	
0~5000		20.1%	0.138	18.3%	0.128	32.7%	0.222	31.2%	0.212	
Average		24.2%	0.165	23.6%	0.161	33.1%	0.224	31.7%	0.215	

Table 14. The SD and ARD of molar excess Gibbs energy and activity of In50Zn50 alloys were estimated by symmetric method at 730 K.

G_m^E and a	Step	MIVM		RSM		Wilson		NRTL		
		ARD%	SD	ARD%	SD	ARD%	SD	ARD%	SD	
G_m^E (J/mol)	0~1000	90.9%	1621	84.0%	1500	98.0%	1750	94.6%	1690	
	1000~2000	113.6%	2029	100.0%	1785	104.7%	1869	99.7%	1781	
	2000~3000	43.9%	784	72.6%	1294	94.0%	1678	89.2%	1594	
	3000~4000	9.6%	178	38.3%	692	82.5%	1472	79.4%	1419	
	4000~5000	10.2%	192	48.9%	868	85.6%	1528	80.6%	1442	
	0~2000	46.4%	824	62.3%	1111	91.8%	1639	88.4%	1579	
	0~3000	60.2%	1070	69.2%	1240	91.8%	1640	89.1%	1592	
	0~4000	42.0%	744	61.4%	1102	89.4%	1597	86.7%	1549	
	0~5000	85.9%	1535	89.4%	1595	100.7%	1798	95.7%	1710	
	Average	55.9%	997	69.6%	1243	93.2%	1663	89.3%	1595	
	a	0~1000	31.3%	0.212	31.2%	0.211	32.9%	0.223	32.4%	0.219
		1000~2000	36.3%	0.246	33.4%	0.226	34.5%	0.233	33.4%	0.226
		2000~3000	17.6%	0.12	29.9%	0.203	32.0%	0.217	30.9%	0.209
3000~4000		5.1%	0.036	24.1%	0.165	29.1%	0.198	28.3%	0.192	
4000~5000		5.7%	0.04	26.2%	0.179	29.9%	0.204	28.6%	0.194	
0~2000		18.5%	0.125	27.9%	0.189	31.4%	0.214	30.8%	0.208	
0~3000		22.9%	0.154	29.3%	0.199	31.4%	0.213	31.1%	0.211	
0~4000		17.0%	0.114	28.1%	0.191	30.8%	0.21	30.4%	0.206	
0~5000		30.0%	0.203	32.1%	0.218	33.6%	0.227	32.5%	0.22	
Average		20.5%	0.139	29.1%	0.198	31.7%	0.215	30.9%	0.21	

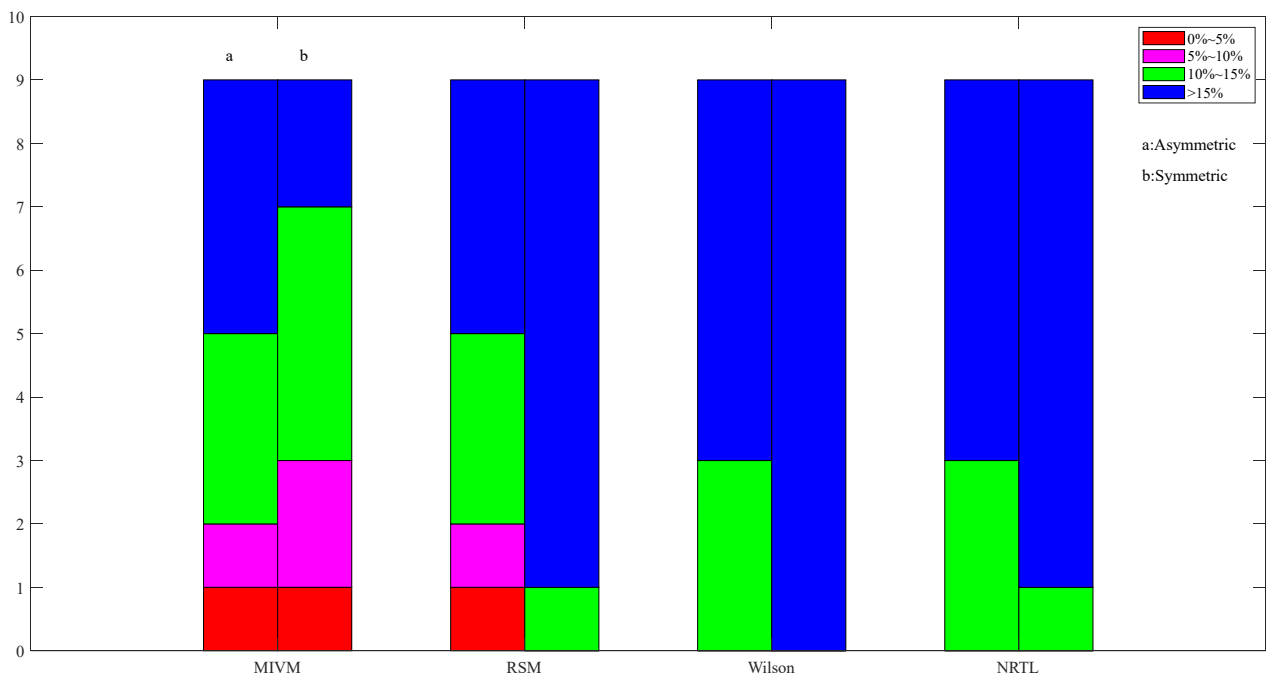


Figure 8. Images of asymmetric and symmetric method activity ARD calculations for Pb50-Sn50 alloys in four models at 1050 K.

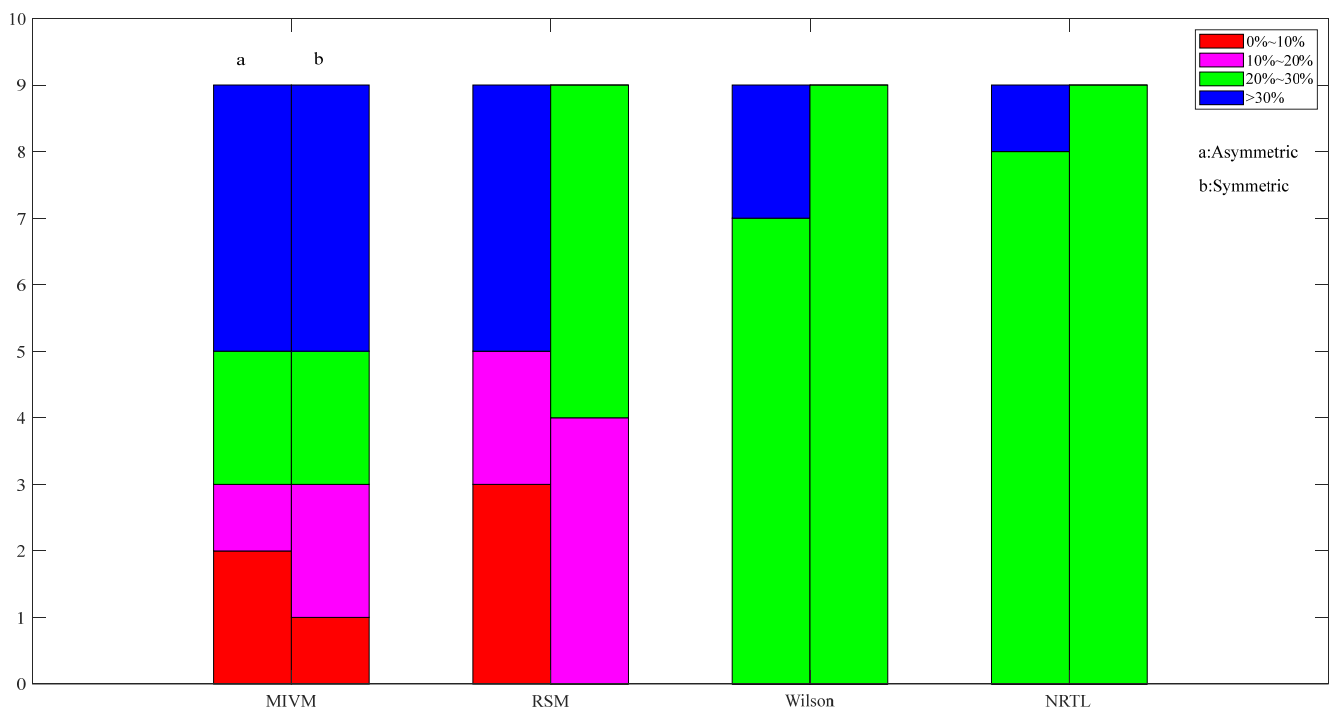


Figure 9. Images of asymmetric and symmetric method activity ARD calculations for Al50-Sn50 alloys in four models at 973 K.

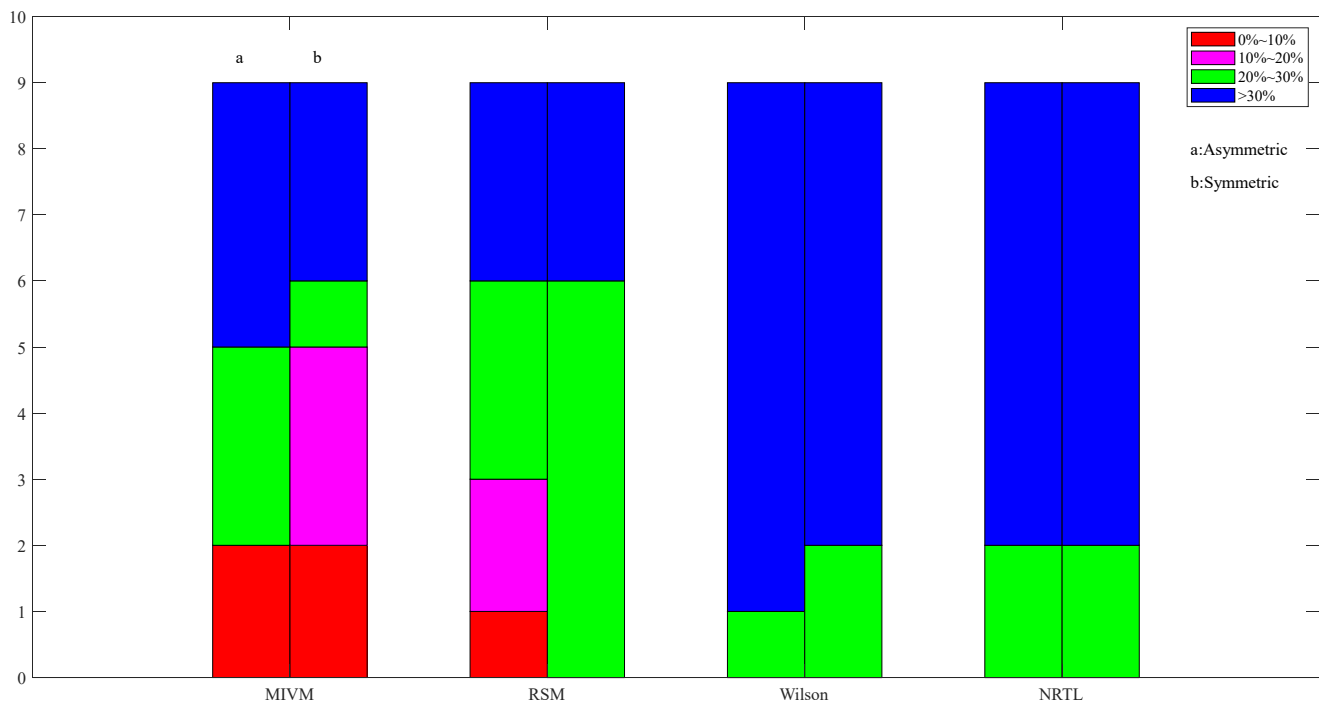


Figure 10. Images of asymmetric and symmetric method activity ARD calculations for In50-Zn50 alloys in four models at 730 K.

5. Conclusions

For the calculation results and comparison of estimating the molar excess Gibbs energy and activity of binary alloys under the Miedema model using the relationship between mixing enthalpy and excess entropy given by Tanaka, Ding, and Sommer (the total ARD of the molar excess Gibbs energy and activity of the three binary liquid alloys under the Miedema model are Tanaka: 3.07% and 8.92%; Ding: 6.09% and 17.1%; Sommer: 4.1% and 14.77%). Preliminary validation of the rationality and feasibility of the Sommer relation for estimating the molar excess Gibbs energy and activity method for binary liquid alloys under the Miedema model. We hope that it can provide a reference for selecting appropriate models and methods to estimate thermodynamic data such as activity and excess Gibbs energy of binary liquid alloys.

Based on the AIMD principle, the kinetic process was simulated by VASP software to obtain the partial radial distribution function of the alloy at different step sizes, and the parameters of MIVM, RSM, Wilson, and NRTL models are calculated by the given pair of the potential energy function and two methods (asymmetric and symmetric methods) to estimate the molar excess Gibbs energy and activity of binary liquid alloys with good rationality and feasibility. The total ARD of the molar excess Gibbs energy and activity of the three binary liquid alloys at full concentration when the PRDF is obtained by the symmetry method are MIVM: 21.59% and 59.35%; RSM: 21.63% and 60.27%; Wilson: 24.27% and 86.7%; NRTL: 23.9% and 83.24%. When the PRDF is obtained by the asymmetric method: MIVM: 22.86% and 68.08%; RSM: 32.84% and 68.66%; Wilson: 25.14% and 82.75%; NRTL: 24.49% and 85.74%. These calculation results show that the ARD for the estimated activity is within reasonable limits, and it is reasonable and feasible to show that this given assumption can be used for the pair potential energy equation for binary liquid alloys. The results also show that the MIVM model performs better than the RSM, Wilson, and NRTL models, and the asymmetric method performs better than the symmetric method. Not all systems are best estimated at the simulation steps from 0 to 5000. This result hopefully provides a research direction for interested researchers (i.e., based on the AIMD principle, the PRDFs obtained from the simulation stepwise calculations by using the VASP software are best fit to the experimental values at which steps).

Author Contributions: Conceptualization, D.T., T.Z. and X.C.; Methodology, D.T.; Theoretical Guidance, D.T.; Review, D.T., X.C., Y.L. and J.H.; Writing—Original Draft, T.Z.; Writing—Review & Editing, T.Z.; Formal analysis, T.Z.; Software, T.Z.; Data Curation, T.Z.; Visualization, T.Z.; Resources, X.C.; Validation, Y.L. and J.H. All authors have read and agreed to the published version of the manuscript.

Funding: This work was financially supported by the National Natural Science Foundation of China under Grant (Grant No. 51464022).

Data Availability Statement: The raw data supporting the conclusions of this article will be made available by the authors on request.

Conflicts of Interest: The authors declare no conflict of interest.

References

1. Chen, L.L.; Li, T.; Zhang, J.P.; Wang, Y.A.; Kong, L.X.; Xu, B.Q.; Yang, B.; Wu, M.Z. Modeling and measurement of vapor-liquid equilibrium of In–Pb and In–Pb–Sn alloy systems in vacuum distillation. *Vacuum* **2023**, *207*, 111556. [\[CrossRef\]](#)
2. Wang, S.P.; Chen, L.L.; Xu, B.Q.; Jiang, W.L.; Kong, L.X.; Yang, B.; Xiong, H.; Qu, C.; Zhang, T.; Zhang, S.H.; et al. Theoretical calculation and experimental investigation on vacuum gasification separation of Ag–Cu–Au ternary alloy. *J. Alloys Compd.* **2023**, *948*, 169685. [\[CrossRef\]](#)
3. Sun, G.Y.; Li, B.; Guo, H.J.; Yang, W.S.; Li, S.Y.; Guo, J. Thermodynamic Study of Energy Consumption and Carbon Dioxide Emission in Ironmaking Process of the Reduction of Iron Oxides by Carbon. *Energies* **2021**, *14*, 1999. [\[CrossRef\]](#)
4. Zhu, Y.Q.; Chen, Z.J.; Zhang, H.M.; Ma, W.H.; Wu, J.J. The effect of Ni on Fe and Al impurities by MIVM model for the silicon production. *Energy* **2022**, *254*, 124459. [\[CrossRef\]](#)
5. Zhao, X.; Cheng, S.X.; Koh, Y.P.; Kelly, B.D.; McKenna, G.B.; Simon, S.L. Prediction of the Synergistic Glass Transition Temperature of Coamorphous Molecular Glasses Using Activity Coefficient Models. *Mol. Pharmaceut.* **2021**, *18*, 3439–3451. [\[CrossRef\]](#)
6. Hildebrande, J.H. The Regular Solution Model for Binary Alloys. *Proc. Natl. Acad. Sci. USA* **1927**, *13*, 267–272.
7. Hildebrand, J.H. Solubility. VIII. Regular Solutions I. *J. Am. Chem. Soc.* **1929**, *1*, 66–80. [\[CrossRef\]](#)
8. Wilson, G.M. Vapor-Liquid Equilibrium. XI. A New Expression for the Excess Free Energy of Mixing. *J. Am. Chem. Soc.* **1964**, *2*, 127–130. [\[CrossRef\]](#)
9. Renon, H.; Prausnitz, J.M. Local compositions in thermodynamic excess functions for liquid mixtures. *Aiche J.* **1968**, *14*, 135–144. [\[CrossRef\]](#)
10. Miedema, A.R. The electronegativity parameter for transition metals: Heat of formation and charge transfer in alloys. *J. Less Common Met.* **1973**, *32*, 117–136. [\[CrossRef\]](#)
11. Miedema, A.R.; Chtel, P.F.; Boer, F.R. Cohesion in alloys—fundamentals of a semi-empirical model. *Phys. B+C* **1980**, *100*, 1–28. [\[CrossRef\]](#)
12. Tao, D.P. A New Model of Thermodynamics of Liquid Mixtures and its Application to Liquid Alloys. *Thermochim. Acta* **2000**, *363*, 105–113. [\[CrossRef\]](#)
13. Zhang, D.; Tang, Y.Z.; Wang, S.; Lin, H.; He, Y. A study on the thermal resistance over metal–carbon nanotube interface by molecular dynamics simulation. *Compos. Interfaces* **2022**, *29*, 899–913. [\[CrossRef\]](#)
14. Zhang, L.; Xiong, D.; Su, Z.; Li, J.; Yin, L.; Yao, Z.; Wang, G.; Zhang, L.; Zhang, H. Molecular dynamics simulation and experimental study of tin growth in SAC lead-free micro solder joints under thermo-mechanical-electrical coupling. *Mater. Today Commun.* **2022**, *33*, 104301. [\[CrossRef\]](#)
15. Surmenev, R.; Grubova, I.Y.; Neyts, E.; Teresov, A.; Koval, N.; Epple, M.; Tyurin, A.; Pichugin, V.; Chaikina, M.; Surmeneva, M.; et al. Ab initio calculations and a scratch test study of RF-magnetron sputter deposited hydroxyapatite and silicon-containing hydroxyapatite coatings. *Surf. Interfaces.* **2020**, *21*, 100727. [\[CrossRef\]](#)
16. Zhuang, C.Q.; Yue, H.; Zhang, H.J. Molecular Simulation Methods and Materials Studio Applications to Macromolecular Material. *Plastics* **2010**, *39*, 81–84. [\[CrossRef\]](#)
17. Kresse, G.; Furthmüller, J. Efficient iterative schemes for ab initio total-energy calculations using a plane-wave basis set. *Phys. Rev. B* **1996**, *54*, 11169. [\[CrossRef\]](#)
18. Boukideur, M.A.; Selhaoui, N.; Alaoui, F.C.; Poletaev, D.; Bouchta, H.; Achgar, K.; Aharoune, A. Thermodynamic assessment of the Ga–Lu system by the combination of ab-initio calculations and the CALPHAD approach. *Calphad* **2022**, *79*, 102464. [\[CrossRef\]](#)
19. Wang, S.Y.; Kramer, M.J.; Xu, M.; Wu, S.; Wang, C.Z. Experimental and ab initio molecular dynamics simulation studies of liquid Al₆₀Cu₄₀ alloy. *Phys. Rev. B* **2009**, *79*, 144205–144209. [\[CrossRef\]](#)
20. Zhang, C.; Wei, Y.; Zhu, C. Structural and electronic properties of liquid InSb alloy: An ab initio molecular-dynamics simulation. *Chem. Phys. Lett.* **2005**, *408*, 348–353. [\[CrossRef\]](#)
21. Tanaka, T.; Gokcen, N.A.; Spencer, P.J.; Morita, Z.I.; Tida, T. Evaluation of interaction parameters in dilute liquid ternary alloys by a solution model based on the free volume theory. *Z. Für Metallkunde* **1993**, *84*, 100–105. [\[CrossRef\]](#)
22. Ding, X.; Wang, W.; Fan, P. Thermodynamic calculation for alloy systems. *Metall. Mater. Trans. B* **1999**, *30*, 271–277. [\[CrossRef\]](#)
23. Witusiewicz, V.T.; Sommer, F. Estimation of the excess entropy of mixing and the excess heat capacity of liquid alloys. *Cheminform* **2001**, *312*, 228–237. [\[CrossRef\]](#)

24. Sommer, F.; Singh, R.N.; Witusiewicz, V. On the entropy of mixing. *J. Alloys Compd.* **2001**, *325*, 118–128. [[CrossRef](#)]
25. Gašior, W.; Moser, Z.; Pstruś, J. Density and surface tension of the Pb–Sn liquid alloys. *J. Phase Equilib. Diff.* **2001**, *22*, 20–25. [[CrossRef](#)]
26. Chikova, O.; Vyukhin, V.; Tsepelev, V. Influence of Melt Superheating Treatment on the Cast Structure of Al–Sn Alloys. *Russ. J. Non-Ferr. Met.* **2021**, *62*, 286–292. [[CrossRef](#)]
27. Pstruś, J.; Moser, Z.; Gašior, W. Surface properties of liquid In–Zn alloys. *Appl. Surf. Sci.* **2011**, *257*, 3867–3871. [[CrossRef](#)]
28. Sun, S.H.; Chen, X.M.; Zhang, F.X.; Yang, B. Ab Initio Molecular Dynamics Simulations of Cu under Vacuum and 473–1573K. *Adv. Mater. Res.* **2013**, 690–693, 2699–2702. [[CrossRef](#)]
29. Mackoy, T.; Kale, B.; Papka, M.E.; Wheeler, R.A. viewSq, a Visual Molecular Dynamics (VMD) module for calculating, analyzing, and visualizing X-ray and neutron structure factors from atomistic simulations. *Comput. Phys. Commun.* **2021**, *264*, 107881. [[CrossRef](#)]
30. Debye, P.; Scherrer, P. *Interferenzen an Regellos Orientierten Teilchen Im Röntgenlicht. I. Nachrichten von der Gesellschaft der Wissenschaften zu Göttingen, Mathematisch-Physikalische Klasse*; Springer: Berlin, Germany, 1916; pp. 1–5.
31. Zernike, F.; Prins, J. Die Beugung Von Röntgenstrahlen in Flüssigkeiten Als Effekt Der Molekülanordnung. *Z. Für Phys. A Hadron. Nuclei.* **1927**, *6*, 184–194. [[CrossRef](#)]
32. Eisenstein, A.; Gingrich, N.S. The Diffraction of X-Rays by Argon in the Liquid, Vapor, and Critical Regions. *Phys. Rev.* **1942**, *62*, 261–270. [[CrossRef](#)]
33. Allen, M.P.; Tildesley, D.J. *Computer Simulation of Liquids*; Oxford University Press: Oxford, UK, 1989; pp. 25–34.
34. Hill, T.L. *Statistical Mechanics: Principles and Selected Applications*; Courier Corporation: Chelmsford, UK, 1957; pp. 185–209.
35. Wang, C.; Chen, X.; Tao, D. Estimation of Component Activities and Molar Excess Gibbs Energy of 19 Binary Liquid Alloys from Partial Pair Distribution Functions in Literature. *Metals* **2023**, *13*, 996. [[CrossRef](#)]
36. Feller, W. *An Introduction to Probability Theory and its Applications*; John Wiley & Sons: Hoboken, NJ, USA, 1950; pp. 220–222.
37. Tao, D.P. The universal characteristics of a thermodynamic model to conform to the Gibbs–Duhem equation. *Sci. Rep.* **2016**, *6*, 35792. [[CrossRef](#)] [[PubMed](#)]
38. Guggenheim, J.A. *Application of Statistical Mechanics*; Clarendon: Oxford, UK, 1966; p. 211.
39. Dorini, T.T.; Eleno, L.T.F. Liquid Bi–Pb and Bi–Li alloys: Mining thermodynamic properties from ab-initio molecular dynamics calculations using thermodynamic models. *Calphad* **2019**, *101687*, 1–9. [[CrossRef](#)]
40. Kubaschewski, O. Metallurgical thermochemistry. *Int. Ser. Mater. Sci. Technol.* **1977**, *24*, 478.
41. Witusiewicz, V.T. Thermodynamics of liquid binary alloys of the 3d transition metals with metalloids: Generalization. *J. Alloys Compd.* **1995**, *221*, 74–85. [[CrossRef](#)]
42. Gokcen, N.A. *Statistical Thermodynamics of Alloys*; Springer Science & Business Media: New York, NY, USA, 1986.
43. Ramesh, B.; Preisser, N.; Michelic, S. Image Processing Procedure to Evaluate Inclusion Dissolution in a Slag Observed by High-Temperature Confocal Scanning Laser Microscopy. *Metals* **2022**, *12*, 531. [[CrossRef](#)]
44. Franke, P.; Neuschütz, D. Binary Systems. Part 3. Binary Systems from Cs–K to Mg–Zr. In *Thermodynamic Properties of Inorganic Materials of Landolt–Börnstein-Group IV Physical Chemistry*; Springer: Berlin, Germany, 2005; Volume 19, pp. 1–3.
45. Franke, P.; Neuschütz, D. Binary Systems. Part 4. Binary Systems from Mn–Mo to Y–Zr. In *Thermodynamic Properties of Inorganic Materials of Landolt–Börnstein-Group IV Physical Chemistry*; Springer: Berlin, Germany, 2006; Volume 19, pp. 1–4.
46. Franke, P.; Neuschütz, D. Binary Systems. Part 5: Binary Systems Supplement 1. In *Thermodynamic Properties of Inorganic Materials of Landolt–Börnstein-Group IV Physical Chemistry*; Springer: Berlin, Germany, 2007; Volume 19, pp. 1–4.

Disclaimer/Publisher’s Note: The statements, opinions and data contained in all publications are solely those of the individual author(s) and contributor(s) and not of MDPI and/or the editor(s). MDPI and/or the editor(s) disclaim responsibility for any injury to people or property resulting from any ideas, methods, instructions or products referred to in the content.